Prediction and Validation of Continuous Fiber Stiffened Plates Manufactured With Continuous Filament Fabrication

by

Nabeel Ahmed Khan

Presented to the Faculty of the Graduate School of

The University of Texas at Arlington in Partial Fulfillment

of the Requirements for the Degree of

MASTER OF SCIENCE IN MECHANICAL ENGINEERING

THE UNIVERSITY OF TEXAS AT ARLINGTON

May 2020

Acknowledgements

Thank you Dr. Robert Taylor, for guiding me through my thesis research and helping me overcome many difficult and unforeseen challenges. Also, I must thank Dr. Ashfaq Adnan and Dr. Andrey Beyle for their support and feedback. Furthermore, I would like to thank my family, particularly my father Ludu Khan, who has supported me from the very beginning, both financially and via encouragement during difficult times.

May 8, 2020

Abstract

Prediction and Validation of Continuous Fiber Stiffened Plates Manufactured With Continuous Fiber Fabrication

Nabeel Ahmed Khan, MS

The University of Texas at Arlington, 2020

Supervising Professor: Robert Taylor

   The purpose of this thesis was to develop an analytical method for predicting the structural properties of continuous fiber stiffened plates, which was then validated both experimentally and via finite element analysis. The MarkForged Mark Two 3D printer enables parts to be printed with continuous carbon fibers embedded within them. A manufacturing process was developed for printing stiffened grids with our without skins, with continuous fiber reinforcement on the top and bottom of the stiffening ribs, which allows bending stiffness can be maximized. An orthotropic grid was printed using Continues Filament Fabrication (CFF), an additive manufacturing process that embeds reinforcing fibers into plastic parts manufactured with Fused Filament Modeling (FFM). The stiffness of this orthotropic grid was then analyzed with laminate plate mechanics. To accomplish this, the results of research conducted by Chen and Tsai was utilized to obtain the stiffness matrices of a grid stiffened plate. Chen-Tsai provided the formulation for the stiffness matrices, allowing the material properties of the carbon fiber and nylon, along with the moment of inertia of the ribs, to be used to calculate the matrices. The stiffness matrices allowed the calculation of bending stiffness, and in turn allowed the deflection to be calculated for a given load. Subsequently, the analytical deflection prediction was

validated via experimental and Finite Element Method analysis. The cantilevered beam experiment provided a result that was very close to the analytical prediction. However the FEM analysis showed significant deviation from the other methods and there was a 50% difference between FEM results and analytical results.

Contents

vi
List of Illustrations

6

List of Tables

1) Introduction

The Markforged Mark Two is a 3D printer that can print composite fiber parts, where the matrix is nylon, and the fiber can be carbon, Kevlar or fiberglass. This printer has two extrusion nozzles in its print head, for nylon and for fiber. The nylon extrusion head prints parts via Fused Filament Fabrication (FFF). The Continuous Fiber Extrusion embeds fiber reinforcement into plastic layers part using carbon fibers, Kevlar or fiberglass. To explore the capabilities of this manufacturing process, a methodology was developed to print stiffened grid structures both with and without skins, then the properties of the grids were evaluated analytically, experimentally and with finite element analysis.
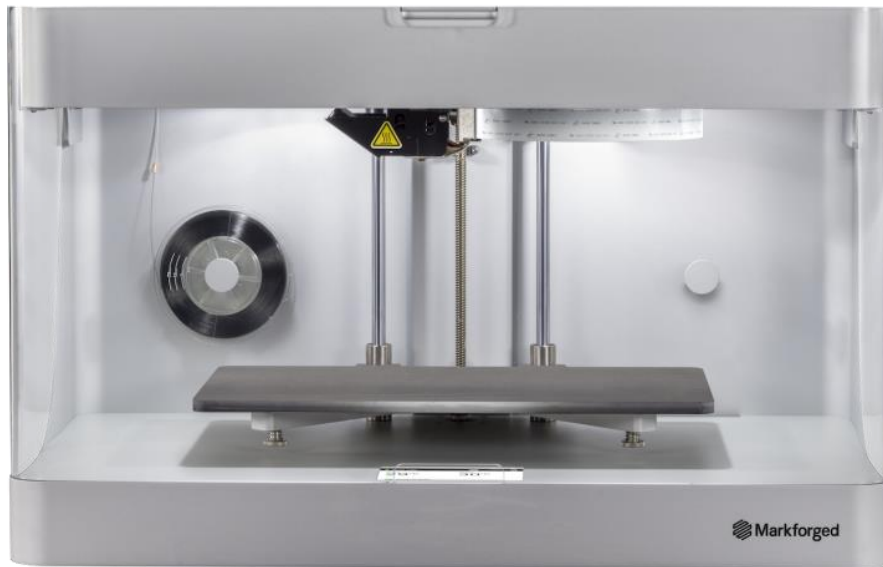
Figure 1 Markforged Mark Two printer [6]

Stiffened panels can be printed with the Markforged mark 2, with or without skin. There is potential for creating lightweight parts in which the fibers are placed exactly where they have the maximum contribution to bending stiffness. In the future, it may be possible to place along optimized directions, where the fibers can follow any arbitrary two dimensional paths. However

there major software limitations right now, which make such precise control fiber placement extremely difficult.

To understand how to use the Mark Two to print stiffened panels, progressively more complex grids were printed. Mistakes, build failures and improper fiber placements were corrected on a trial and error basis. The fibers had to be placed on the top and bottom of the ribs, in order to maximize bending stiffness. Furthermore, in order to reduce mass, it had to be determined how thin the dimensions of the walls could be. The specific software options that allowed for single bead thick walls and specific fiber angles needed to be understood. However there were many difficulties due to print failures, which included burnt parts, delamination between layers, curling and bad surface finish.

An analytical procedure to determine the behavior of the grids was developed using laminated plate theory. The moments of inertia of each rib were first calculated, then the Tsai-Chen equations were used to calculate the rib stiffness matrices [1]. Then, from the PHD dissertation of Rios [4] an equation was found to calculate deflection from the stiffness matrices.

FEM analysis was also performed using thin skin to represent nylon sections and one dimensional rods to represent carbon. The results didn't match but they had the same order of magnitude. Finally, experiments were performed to see what the real life performance of the parts were. The cantilevered beam deflection experiments produced results that agreed very closely with the analytical deflection predictions.

2) Background

The ability to manufacture parts with continuous strands of carbon fiber can be taken advantage of to produce strong, stiff composite grids that are also light. Furthermore, carbon nylon composites have the potential to be tough and impact resistant, unlike most carbon fiber parts with epoxy matrix, which are brittle. Grids tend to be damage resistant because they do not delaminate, and cracks do not propagate between ribs due to empty space. The design process for continuous filament fabrication is the same as fused filament fabrication for the most part. However, certain considerations must be taken for making sure fiber placement is correct. For example, thin geometry must have a minimum width on order to allow fibers to be within them, correct setting must be used in order to avoid errors such as fiber curling or discontinuity.

The behavior of thin panels must be understood in order to know how to stiffen them. A thin panel buckles when loading exceeds a critical value and this value changes depending upon the length of the thin plate and its thickness. Grids can be placed on a thin plate to break it up into smaller segments with much smaller lengths, and furthermore the ribs of the grid also add to the stiffness of the overall structure by reacting to loads.

An equivalent stiffness model was used to analyze a laminated orthotropic grid. Such models are easy to use and simple to script with a programming language. Tsai and Chen used an equivalent stiffness model to develop an extension of laminate plate theory that would apply to grid stiffened structures [2].

Altair Optistruct was used to analyze an idealized model where it was assumed that the thin nylon skin segments were modelled with thin skin and the carbon segments were modelled as one dimensional rods.

2.1) Continuous Filament Fabrication

The Markforged Mark Two 3d printer is a double nozzle additive manufacturing tool. There is a nylon extrusion nozzle that can print plastic parts using the FFF process. There is a second nozzle that is used to lay down continuous strands of carbon fiber into the nylon, thereby stiffening the part. Although there are limitations in the software, the Mark Two is capable of laying down fiber in specific directions and therefore, there is potential for tailoring stiffness properties for specific requirements. One potential use for this printer is to construct grid stiffened panels, where the carbon fiber is placed at the top and bottom of the stiffening ribs. The carbon fiber can be placed at the top and bottom of the ribs to maximize bending stiffness.
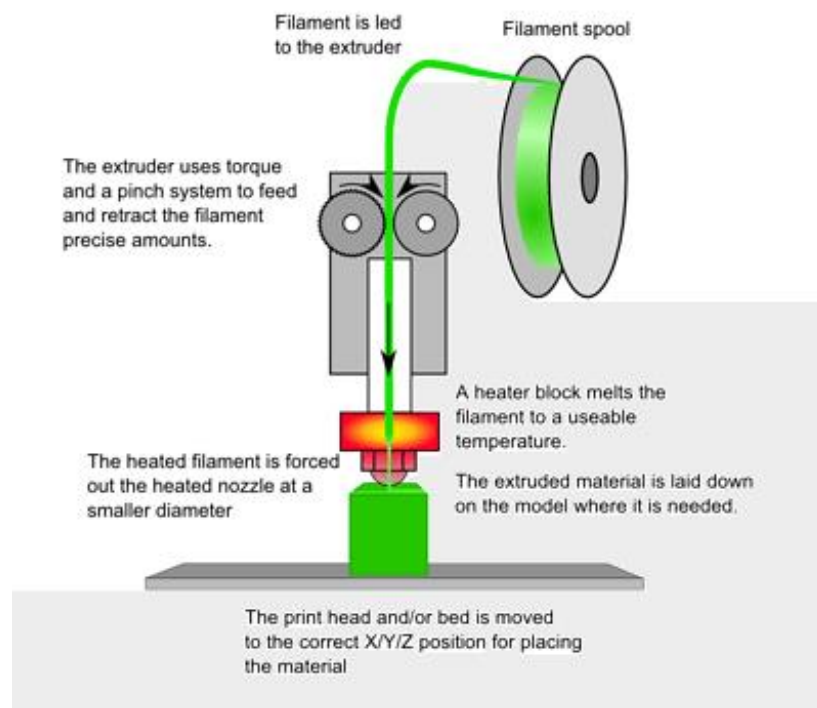
Figure 2 FFM Process Diagram [7]

The Fiber Filament Fusion (FFF) process manufactures part by depositing heated plastic onto successive layers, where each layer fuses with a previous layer, until the whole part is formed [6]. The plastic is supplied to the heated nozzle as a solid filament that is stored near the printer in a

spool. The spool itself is stored in a separate container that is sealed and has silica gel packs to reduce moisture contamination of the nylon spool.
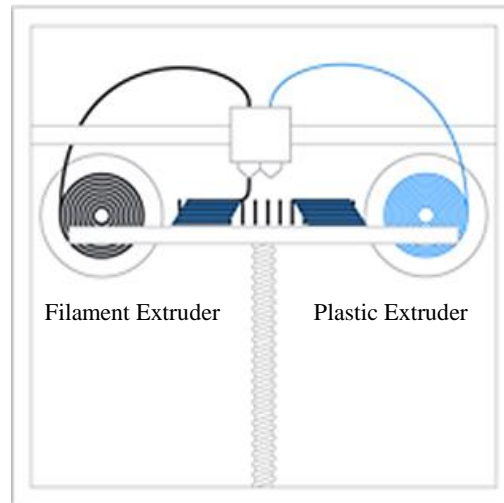
Figure 3 CFF Diagram   [6]

The Continuous Filament Fabrication (CFF) process supplements the FFF process embedding continuous fiber into a part [6]. This is done with a second nozzle that heats up the fiber and pushes into a previously printed layer of nylon. Thus the nylon layers printed with the FFF process becomes the matrix into which fibers are embedded with the CFF process, enabling composite parts to be printed.

The combination of nylon layers with embedded carbon fiber results in a composite material. This material has a nylon matrix, which bonds the carbon fibers together, which in turn resist structural loads. Composite materials have different properties compared to their constituent materials. In the case of carbon nylon composite, the heated nylon bonds easily to both other nylon layers, and to the carbon. Compared to carbon fiber strands, the FFF printed nylon can withstand much higher strains, and endure significant plastic deformation before ultimate failure. By contrast, carbon fiber is brittle and breaks easily at very low strains, and does not undergo

appreciable plastic deformation before failure. However, it is much stiffer than nylon when subjected to tensile loads.

To find the material properties of the matrix and fiber, the Markforged Materials Datasheet 2017 was referenced [8]. For the purposes of the stiffened grids research, the most important properties were the Young's moduli of the materials. For nylon, Young's Modulus is 0.94 GPa, and 54 GPa for carbon fiber. Thus it can be seen by simple division, that the carbon fiber is approximately 57 times stiffer than the nylon matrix. Therefore the stiffness of the carbon dominates the stiffness of the nylon, and provides the majority of the stiffness for composite parts that are printed with the Mark Two.

Furthermore it should be noted that the ability of the Markforged Mark Two to print parts with continuous carbon fibers, is unique to Markforged printers. Each fiber is stiff in tension, but has no resistance to compression or shear. However, when many fibers are bonded together within the nylon matrix, they can work together to resist loads, which becomes distributed continuously over the length of the fibers. Thus, the Mark Two printer can produce parts that have the potential to be much stiffer that alternative FFF printers, which use discontinuous (chopped) fibers within plastic filaments.

2.2) Designing for CFF

As previously stated, Continuous Filament Fabrication (CFF) is an extension of Fused Filament Fabrication (FFM), ie CFF extends the capabilities of FFM by supplementing the strength of FFM manufactured plastics by embedding continuous fibers into the part to contribute structural stiffness. To design strong, stiff parts for a given loading condition, with acceptable surface finish and dimensional accuracy, certain considerations should be made during the design phase. Amongst these considerations are anisotropy, supports for bridges and overhangs, infill percentage and geometry, and the thickness of roof, wall and floor layers.

FFM manufactured parts are anisotropic, meaning that the parts have different strength/stiffness properties along different directions. An FFM printed part is weakest perpendicular to bead direction, (vertical to the printed layers) due to individual layers being bonded to each other. If loaded vertical to bead direction, the bond between the layers is loaded in tension, and the bond is weaker than the isotropic strength of the base material being printed.

Vertical Forces   Horizontal Forces
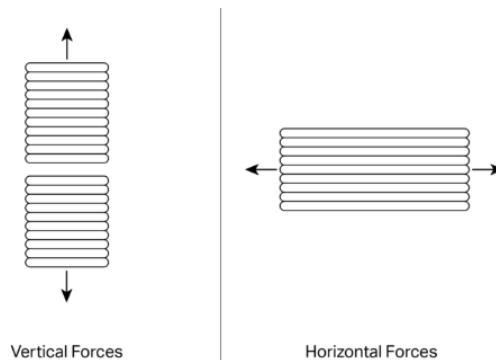
Figure 4 Loading Direction vs Bead direction   [10]

An FFM printed part is much stronger along the bead directions. Therefore, a part should be designed such that tension, compression or bending loads result in normal stresses that resolve along the longitudinal axes of the beads. Furthermore, when being printed, the part has to be oriented appropriately.

Another factor to be accounted for while designing an FFF part, is supports. Supports are needed to print bridges and overhangs. Bridges occur when material must be printed between gaps, such as between two upright walls. The material in bridges tend to sag downwards due to weight. However if supports are printed between gaps, the bridge distance decreases, reducing the sagging tendency or effectively eliminating it if the gap between supports is small enough. Overhangs occur when surfaces are sloped such that previously printed layers do not fully support layers that are printed later. If the overhang is relatively upright (rule of thumb is less than 45 degrees of slope) then usually be it can be printed without many problems. However, if the overhang is long and deep, then there may be a number of printing issues, including bad bonding between layers, curling, bulging or bad surface finish. Supports help when printing overhangs by reducing the amount of material that is not constrained by the previously printed layers. After printing is finished supports can be removed from the final part.

The infill is the internal structure of a printed part. A printed part does not need to be a solid block of material, it can have empty space internally. In most cases, it is desirable to minimize material usage and maximize air pockets within an FFM manufactured part. This results in less material usage, lower print time and reduced weight. The infill is characterized by the layout of internal structural members and the percentage of volume occupied by material.

Infill structure can have many variants, however the default options available for the Mark Two are rectangular, triangular and hexagonal infill (along with solid parts). Furthermore, Eiger automatically decides percentage of infill that is allowable for any given part being sliced. For triangular and hexagonal infill, Eiger determines a recommended infill percentage, and a range of allowable infill percentages (the internal algorithm for determining these percentages is not known). In such cases, Eiger does not allow infill percentage that is higher or lower than the

allowable. However, for rectangular infill, any required infill percentage can be used, and the Eiger recommendations can be overridden.
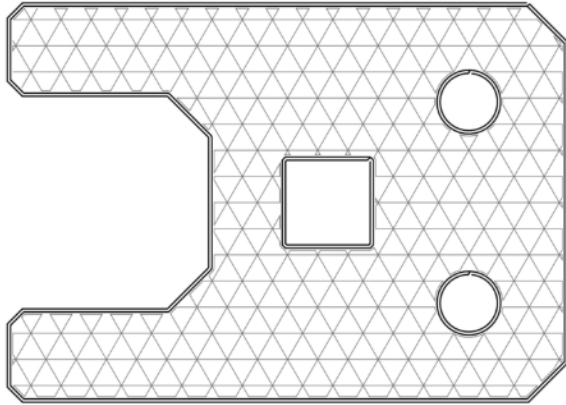
Figure 5 Triangular Infill [10]
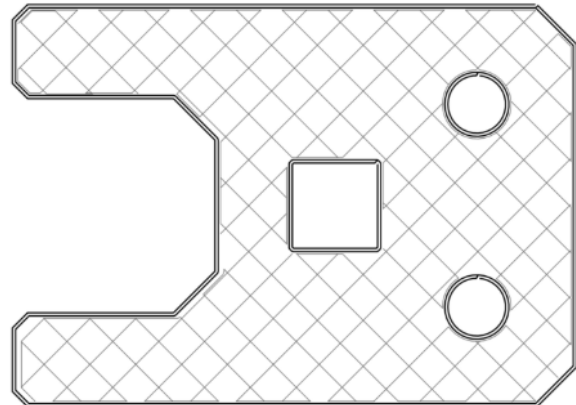
Figure 6 Rectangular Infill [10]
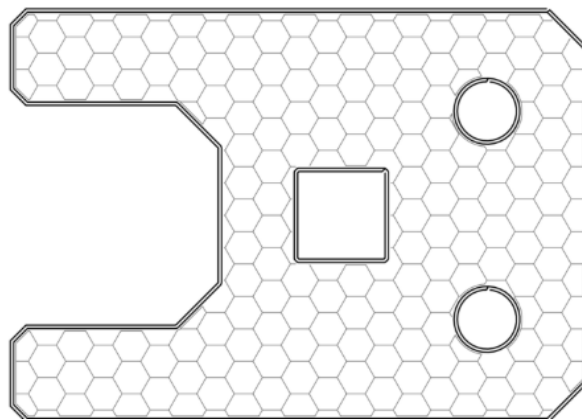
Figure 7 Hexagonal infill [10]

For the Mark Two printer, Markforged recommends certain limitations for the print settings. Roof and floor layers are recommended to be at least four layers thick (0.5mm), where each layer is 0.125mm thick. Also, the thickness of walls are recommended to be a minimum of two layers. A single layer was measured to be 0.65mm thick, thus the minimum recommended thickness is 1.3mm. However, it is possible to print thinner layers than the manufacturer recommended layers, albeit with the risk of print failures. Parts are also subject to significant shrinkage and warping.

2.3) Stiffened Plates

Consider a plate under distributed loading $q(x,y)$. The shows diagram a three dimensional coordinate system, with axes labeled x, y and z. The longitudinal axis is x, the lateral axis is y and z is the vertical axis. The length of the plate is a, width is b and the thickness is t. There is a uniformly distributed load applied along the x axis, across the thickness of the plate, N_x (per unit length). Assume the plate to be simply supported along all four edges.
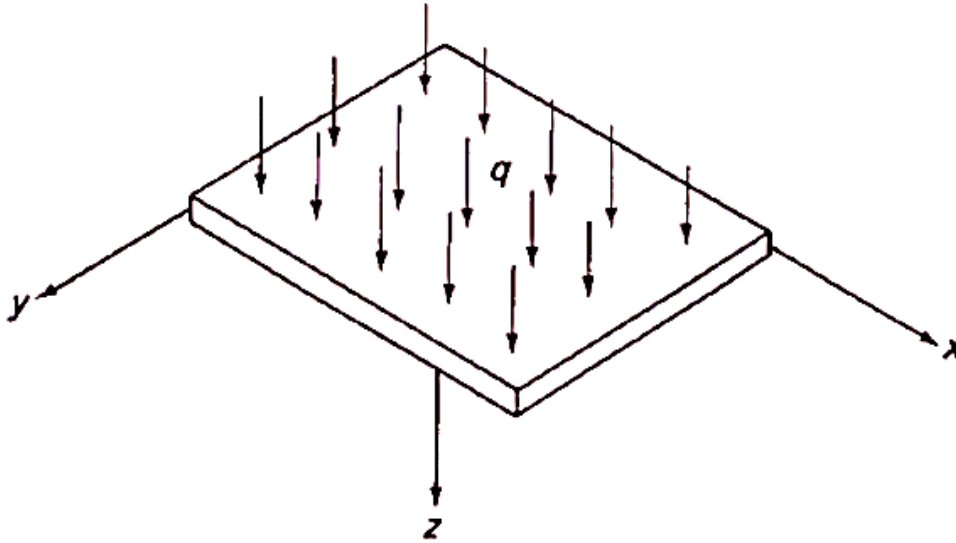
Figure 8   Thin Plate under buckling load [11, pp.129]

The deflected shape of the loaded plate can be determined by solving the differential equation for $w(x,y)$ [11, pp. 131]:

$$(\nabla^2)^2 w = \frac{q}{D}$$

The symbol D represents the flexural rigidity of the plate and it given by the following equation [11, pp. 124], where E is Young's Modulus, t is plate thickness and v is Poisson's constant:

$$D = \frac{E\,t^3}{12(1-v)}$$

To solve the differential equation, the boundary conditions of the simply supported plate must be considered. These boundary conditions must be determined at the extreme ends of the plate, but since a thin plate is considered (planar problem), conditions along the z axis can be neglected. The boundary conditions to be applied are:

$$w(x, y) = 0 \ and \ \frac{\partial^2 w}{\partial x^2} = 0 \ at \ x = 0, a$$

$$w(x, y) = 0 \ and \ \frac{\partial^2 w}{\partial x^2} = 0 \ at \ y = 0, b$$

Deflection and load can be represented as a Fourier series. The coefficients m and n are integers that represent the number of half wavelengths of the deformed shape, in x and y axes respectively. The coefficient A_{mn} and a_{mn} are unknown and must be determined.

$$w(x, y) = \sum_{m=1}^{\infty} \sum_{n=1}^{\infty} A_{mn} \sin(\frac{m\pi}{a} x) \sin(\frac{n\pi}{b} y)$$

$$q(x, y) = \sum_{m=1}^{\infty} \sum_{n=1}^{\infty} a_{mn} \sin(\frac{m\pi}{a} x) \sin(\frac{n\pi}{b} y)$$

Substituting the Fourier series representations of $w(x,y)$ and $q(x,y)$ into the differential equation and arranging it to equal zero:

$$\sum_{m=1}^{\infty} \sum_{n=1}^{\infty} \{A_{mn} \left[\left(\frac{m\pi}{a}\right)^4 + 2\left(\frac{m\pi}{a}\right)^2 \left(\frac{n\pi}{b}\right)^2 + \left(\frac{n\pi}{b}\right)^4 \right] - \frac{a_{mn}}{D} \} \sin(\frac{m\pi}{a} x) \sin(\frac{n\pi}{b} y) = 0$$

The equation is valid for all values of x and y, and because it equals zero we can write:

$$A_{mn} \pi^4 \left(\frac{m^2}{a^2} + \frac{n^2}{b^2} \right)^2 - \frac{a_{mn}}{D} = 0$$

This equation can be arranged to solve for A_{mn}:

$$A_{mn} = \frac{\pi^4}{D} \frac{a_{mn}}{\left(\frac{m^2}{a^2} + \frac{n^2}{b^2}\right)^2}$$

For specific values of m and n coefficient $a_{mn\backslash}$ can be found via integration:

$$a_{mn} = \frac{4}{ab} \int_0^a \int_0^b a_{mn} \sin(\frac{m\pi}{a}x) \sin(\frac{n\pi}{b}y) \ dx \ dy$$

For simplification, assume that load is uniformly distributed, the $q(x,y) = q_0$ and that the plate

is square, thus $a=b$. Maximum displacement occurs in the middle of the plate, where $x=y= a/2$.

These simplifications result in:

$$a_{mn} = \frac{16 \ q_0}{\pi^2 mn}$$

Which can be substituted into the equation for $w(x,y)$ with $x=y= a/2$, to get w_{max} :

$$w_{max} = \frac{16 \ q_0}{\pi^6 D} \sum_{m=1}^{\infty} \sum_{n=1}^{\infty} \frac{(\sin(\frac{m\pi}{2}) \sin(\frac{n\pi}{2})}{mn \left(\frac{m^2}{a^2} + \frac{n^2}{a^2}\right)^2}$$

For further simplification, it should be noticed that the w_{max} becomes zero when m or n are even

(or if both are even). Also, the summation converges very quickly, so only the first four odd

numbered terms need to be considered. Thus, the summation should be performed for $m = 1,3,5,7$

and $n = 1,3,5,7$. This results in w_{max} being simplified to:

$$w_{max} = \frac{16 \ q_0}{\pi^6 D} a^4 \ (0.2441)$$

Substituting the formula for D (flexural rigidity):

$$w_{max} = \frac{16 \ q_0}{\pi^6} \frac{12(1 - v^2)}{Et^3} a^4 (0.2441)$$

Thus for a square, simply supported plate with uniformly distributed loading, maximum deflection is:

$$w_{max} = 0.0487 \frac{(1 - v^2)}{E} \frac{a^4}{t^3}$$

From the equation for maximum deflection, it can be seen that w_{max} is proportional to the fourth power of length a, and is inversely proportional to the third power of thickness t. Thus for a given thickness, to decrease the maximum deflection (and effectively increase plate stiffness), the width and length dimensions could be shortened.
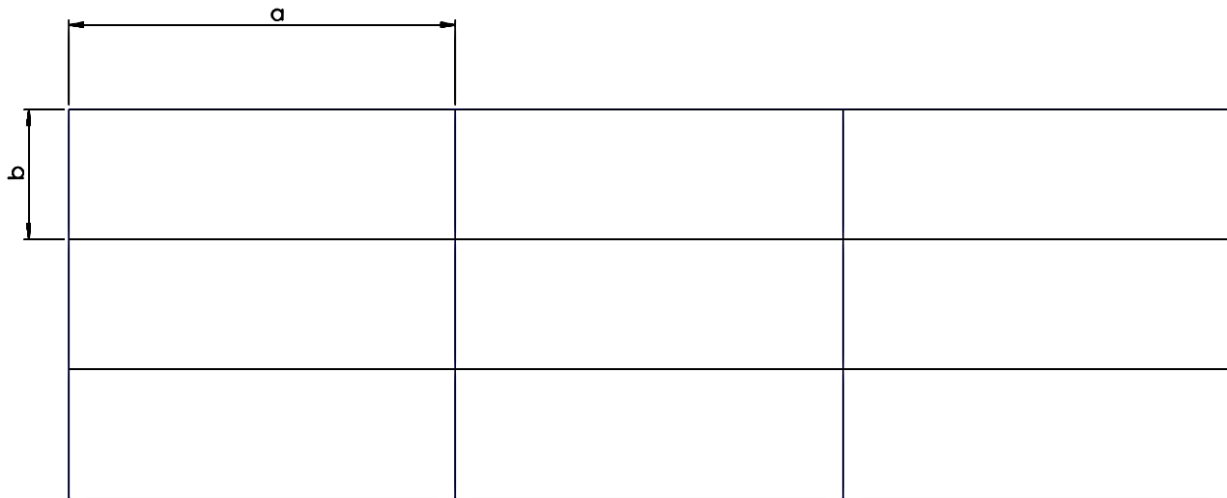
Figure 9 Stiffening Grid

A grid of stiffeners may be placed on the surface of a thin plate. The plate will therefore be divided into subsections, each of which would act like a smaller plate. Furthermore, longitudinal stiffeners can support axial stresses, which further increase critical load.

However, this simple explanation of stiffened plates is not entirely valid for parts printed with the Markforged Mark Two, because the plates end up being non isotropic, laminated plates. While the fundamental physics remain the same (by dividing into subsections and taking advantage of the stiffener to react to loads), analysis and prediction must take into account laminated plate mechanics.

2.4) Laminate Plate Theory
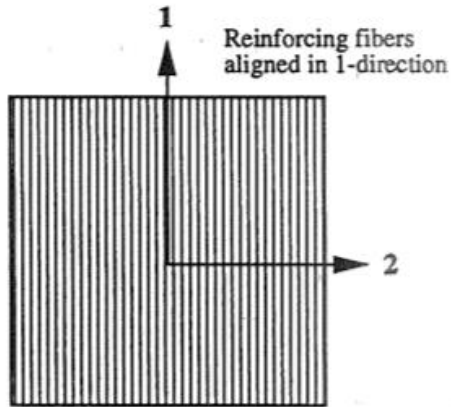
Figure 10 Orthotropic Plate [3]

Consider a 2d orthotropic plate with reinforcing fibers.

Vertical stiffness is different from horizontal stiffness, thus:

$$E1 = \frac{\sigma 1}{\varepsilon 1}$$

$$E2 = \frac{\sigma 2}{\varepsilon 2}$$

$$\tau 12 = \gamma 12 \, G12$$

Poisson's ratio also varies between the two directions. Thus:

$$v12 = \frac{\varepsilon 1}{\varepsilon 2}$$

$$v21 = \frac{\varepsilon 2}{\varepsilon 1}$$

Furthermore, there is a relation between Poisson's ratio and Young's moduli in each direction:

$$v21 \, E1 = v21 \, E2$$

$$\text{thus,} \ \frac{v21}{E2} = \frac{v12}{E1}$$

Using the Young's Modulus and Poisson's ratio we can write equations for strain:

$$\epsilon 1 = \frac{\sigma 1}{E1} - v21 \frac{\sigma 2}{E2}$$

$$\epsilon 2 = \frac{\sigma 2}{E2} - v12 \frac{\sigma 1}{E1}$$

Written in a matrix format this becomes:

$$\begin{bmatrix} \varepsilon 1 \\ \varepsilon 2 \\ \gamma 6 \end{bmatrix} = \begin{bmatrix} \dfrac{1}{E1} & -\dfrac{v21}{E2} & 0 \\ -\dfrac{v12}{E1} & \dfrac{1}{E2} & 0 \\ 0 & 0 & \dfrac{1}{G12} \end{bmatrix} \begin{bmatrix} \sigma 1 \\ \sigma 2 \\ \tau 6 \end{bmatrix}$$

This can be rewritten as:

$$\begin{bmatrix} \varepsilon 1 \\ \varepsilon 2 \\ \gamma 6 \end{bmatrix} = \begin{bmatrix} S11 & S12 & 0 \\ S12 & S22 & 0 \\ 0 & 0 & S66 \end{bmatrix} \begin{bmatrix} \sigma 1 \\ \sigma 2 \\ \tau 6 \end{bmatrix}$$

Where:

$$\text{S11} = \frac{1}{E1}, \text{S12} = -\frac{v21}{E2}, \text{S21} = -\frac{v12}{E1} = \text{S12}, \text{S66} = \frac{1}{G12}$$

In short, we can write:

$$[\varepsilon] = [S][\,\sigma\,]$$

[S] is called the compliance matrix. The inverse of the compliance matrix is the reduced stiffness matrix [Q].

$$[Q] = [S]^{-1}$$

$$[Q] = \begin{bmatrix} Q11 & Q12 & 0 \\ Q12 & Q22 & 0 \\ 0 & 0 & Q66 \end{bmatrix}$$

Where:

$$\text{Q11} = \frac{E1}{1 - v12\,v21}, \text{Q12} = \text{Q21} = \frac{E1}{1 - v12\,v21}, \text{Q66} = \text{G12}$$

Therefore, the stress strain relation can be written as:

$$\begin{bmatrix} \sigma 1 \\ \sigma 2 \\ \tau 6 \end{bmatrix} = \begin{bmatrix} Q11 & Q12 & 0 \\ Q12 & Q22 & 0 \\ 0 & 0 & Q66 \end{bmatrix} \begin{bmatrix} \varepsilon 1 \\ \varepsilon 2 \\ \gamma 6 \end{bmatrix}$$
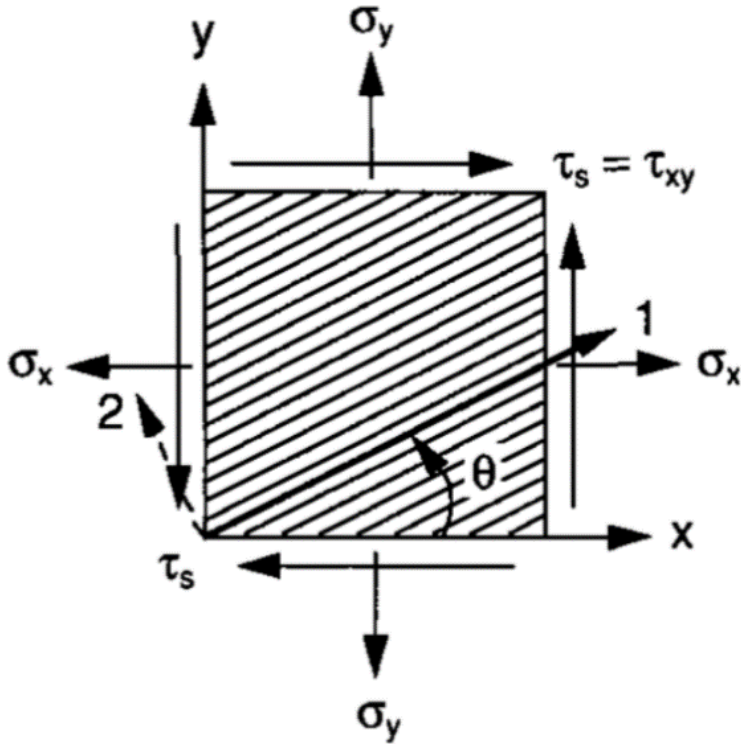
Figure 11 2D Laminate Stress Cube [3]

Now consider a 2D stress cube. Let x and y be the global coordinate axes. The stress along the horizontal axis is σ_x and along vertical axis it is σ_y. Shear stress is τ_s. There is a second coordinate system, rotated counter clockwise relative to xy by angle θ, and the two axes are labeled 1 and 2. The stresses in global coordinates can be converted into stresses along the rotated axes.

A transformation matrix needs to be used and this is stated in the Daniel and Ishai reference[3] to be:

$$[T] = \begin{bmatrix} m^2 & n^2 & -2mn \\ n^2 & m^2 & 2mn \\ mn & -mn & m^2 - n^2 \end{bmatrix} \quad m = \cos(\theta),\ n = \sin(\theta)$$

The T matrix can be used to convert the stress and strains to the rotated axes using the equations:

$$\begin{bmatrix} \sigma 1 \\ \sigma 2 \\ \tau 6 \end{bmatrix} = [T] \begin{bmatrix} \sigma x \\ \sigma y \\ \tau z \end{bmatrix}$$

$$\begin{bmatrix} \varepsilon 1 \\ \varepsilon 2 \\ \frac{1}{2}\gamma 6 \end{bmatrix} = [T] \begin{bmatrix} \varepsilon x \\ \varepsilon y \\ \frac{1}{2}\gamma s \end{bmatrix}$$

The ½ constant was introduced for convenience in order to allow the same [T] matrix to be used for transforming both the stress and the strain matrices.

Now consider a section of a laminate plate, shown before and after deformation. The center of the laminate is the reference plane, which is assumed to experience no strain after the deformation.
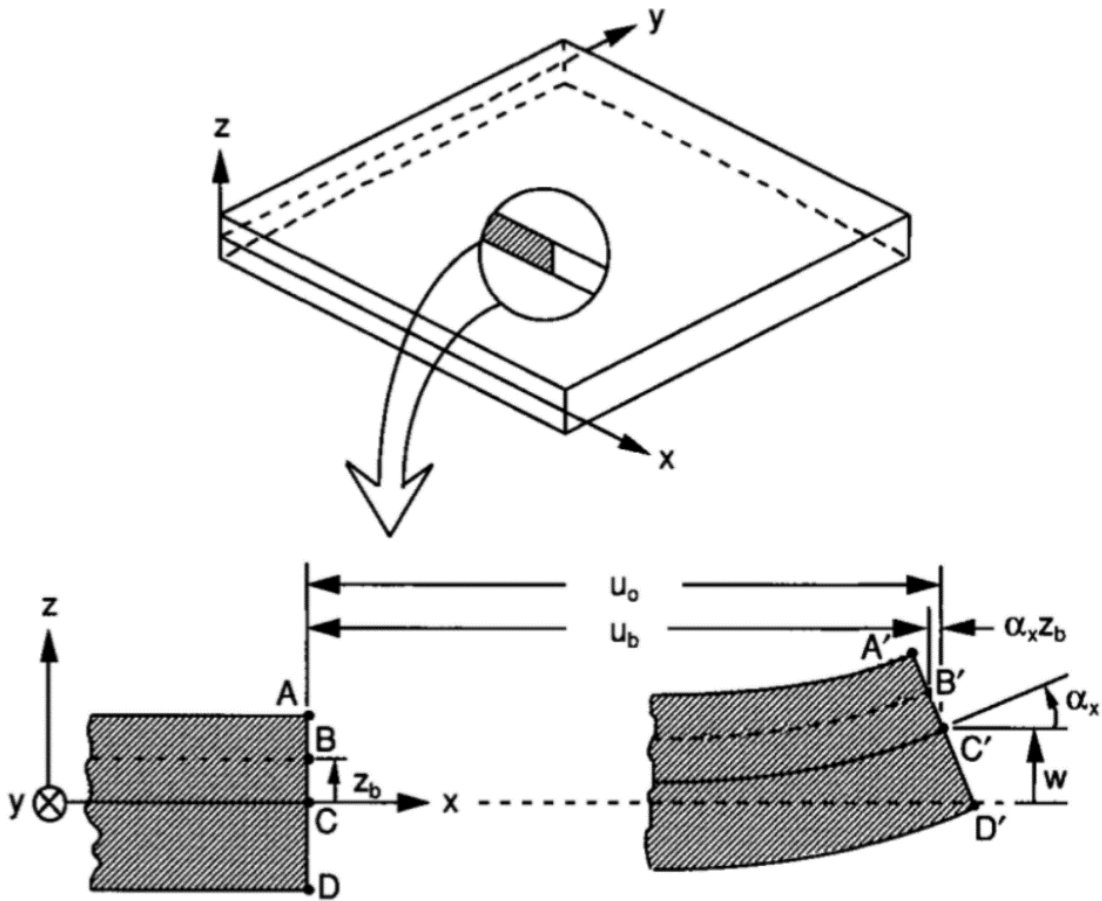
Figure 12 Laminate Section, pre and post Deformation [3]

Displacements of the reference plane in *x* and *y* dimensions are:

$$u_0 = u_0(x,y)$$

$$y_0 = v_0(x,y)$$

Out of plane displacement occurs along the z axis and is described by:

$$w = f(x,y)$$

The x and y axis rotations are:

$$\alpha_x = \frac{\partial w}{\partial x}$$

$$\alpha_y = \frac{\partial w}{\partial y}$$

The curvatures of the laminate are:

$$\kappa_x = -\frac{\partial^2 w}{\partial x^2}$$

$$\kappa_y = -\frac{\partial^2 w}{\partial y^2}$$

$$\kappa_{xy} = \kappa_s = -2\frac{\partial^2 w}{\partial x \partial y}$$

In the diagram, point B has a displacement of z_b along the z axis. After bending the displacement components of point B are:

$$u_b = u_0 - \alpha_x z_b$$

$$v_b = v_0 - \alpha_y z_b$$

For any arbitrary point along the cross section of the lamina, the equations for the rotations can be substituted into the above relations and z_b can be substituted with the z axis displacement for any required point, and we can obtain:

$$u_b = u_0 - z\frac{\partial w}{\partial x}$$

$$v_b = v_0 - z\frac{\partial w}{\partial y}$$

These displacement relations can be used to obtain strain relations, by using the classical elasticity strain displacement partial differential equations.

$$\varepsilon_x = \frac{\partial u}{\partial x} = \frac{\partial u_0}{\partial x} - z\,\frac{\partial^2 w}{\partial x^2}$$

$$\varepsilon_y = \frac{\partial v}{\partial x} = \frac{\partial v_0}{\partial y} - z\,\frac{\partial^2 w}{\partial y^2}$$

$$\gamma_{xy} = \gamma_s = \frac{\partial u}{\partial y} + \frac{\partial v}{\partial x} = \frac{\partial u_0}{\partial y} + \frac{\partial v_0}{\partial x} - 2z\frac{\partial^2 w}{\partial x \partial y}$$

Observe that the reference plane strain components can be written as:

$$\varepsilon_x^0 = \frac{\partial u_0}{\partial x}$$

$$\varepsilon_y^0 = \frac{\partial v_0}{\partial y}$$

$$\gamma_{xy}^0 = \gamma_s^0 = \frac{\partial u_0}{\partial y} + \frac{\partial v_0}{\partial x}$$

The strain components on the reference plane and the curvatures of the laminates can be substituted into the strain-displacement equation:

$$\varepsilon_x = \frac{\partial u}{\partial x} = \varepsilon_x^0 + z\,\kappa_x$$

$$\varepsilon_y = \frac{\partial v}{\partial x} = \varepsilon_y^0 + z\,\kappa_y$$

$$\gamma_{xy} = \gamma_s = \frac{\partial u}{\partial y} + \frac{\partial v}{\partial x} = \gamma_s^0 + z\kappa_s$$

Written as matrices we obtain:

$$\begin{bmatrix} \varepsilon_x \\ \varepsilon_y \\ \gamma_s \end{bmatrix} = \begin{bmatrix} \varepsilon_x^0 \\ \varepsilon_y^0 \\ \gamma_s^0 \end{bmatrix} + z \begin{bmatrix} \kappa_x \\ \kappa_y \\ \kappa_s \end{bmatrix}$$

27

Thus the stress strain relation can be written as:

$$\begin{bmatrix} \sigma_x \\ \sigma_y \\ \tau_s \end{bmatrix} = \begin{bmatrix} Q_{xx} & Q_{xy} & 0 \\ Q_{yx} & Q_{yy} & 0 \\ 0 & 0 & Q_{ss} \end{bmatrix} \begin{bmatrix} \varepsilon_x \\ \varepsilon_y \\ \gamma_s \end{bmatrix} = \begin{bmatrix} Q_{xx} & Q_{xy} & 0 \\ Q_{yx} & Q_{yy} & 0 \\ 0 & 0 & Q_{ss} \end{bmatrix} \left(\begin{bmatrix} \varepsilon_x^0 \\ \varepsilon_y^0 \\ \gamma_s^0 \end{bmatrix} + z \begin{bmatrix} \kappa_x \\ \kappa_y \\ \kappa_s \end{bmatrix} \right)$$

$$\begin{bmatrix} \sigma_x \\ \sigma_y \\ \tau_s \end{bmatrix} = \begin{bmatrix} Q_{xx} & Q_{xy} & 0 \\ Q_{yx} & Q_{yy} & 0 \\ 0 & 0 & Q_{ss} \end{bmatrix} \begin{bmatrix} \varepsilon_x^0 \\ \varepsilon_y^0 \\ \gamma_s^0 \end{bmatrix} + z \begin{bmatrix} Q_{xx} & Q_{xy} & 0 \\ Q_{yx} & Q_{yy} & 0 \\ 0 & 0 & Q_{ss} \end{bmatrix} \begin{bmatrix} \kappa_x \\ \kappa_y \\ \kappa_s \end{bmatrix}$$

Now consider a single laminate layer under loading, with normal forces Nx and Ny, shear for Ns and moments Mx, My and Ms. Thickness of the layer is t. Normal forces are:
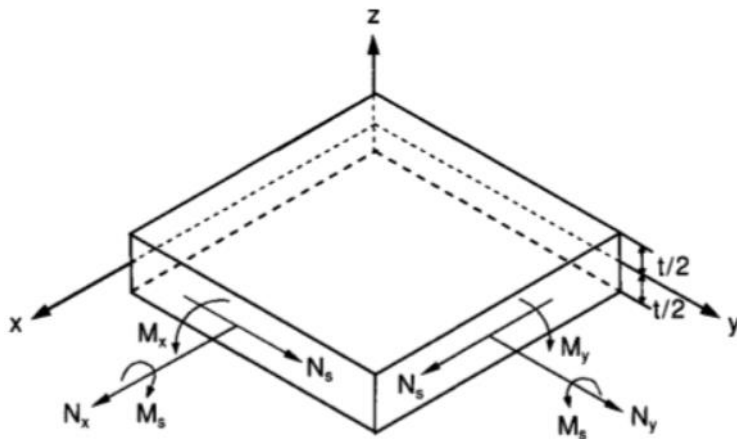
$$N_x^k = \int_{-\frac{t}{2}}^{\frac{t}{2}} \sigma_x \, dz$$

$$N_x^k = \int_{-\frac{t}{2}}^{\frac{t}{2}} \sigma_y \, dz$$

$$N_s^k = \int_{-\frac{t}{2}}^{\frac{t}{2}} \tau_s \, dz$$

Figure 13 Force and Moment Resultants on Single Layer Element [3]

The superscript k denotes that the relations apply to a specific layer within the laminate, also labeled k. The expressions for moment are similar:

$$M_x^k = \int_{-\frac{t}{2}}^{\frac{t}{2}} \sigma_x \, z dz$$

$$M_y^k = \int_{-\frac{t}{2}}^{\frac{t}{2}} \sigma_x \, z dz$$

$$M_s^k = \int_{-\frac{t}{2}}^{\frac{t}{2}} \tau_s z \, dz$$

28

Writing the integral equations as matrices:

$$
\begin{bmatrix} N_x^k \\ N_y^k \\ N_s^k \end{bmatrix} = \int_{-\frac{t}{2}}^{\frac{t}{2}} \begin{bmatrix} \sigma_x \\ \sigma_y \\ \tau_s \end{bmatrix} dz
$$

$$
\begin{bmatrix} M_x^k \\ M_y^k \\ M_s^k \end{bmatrix} = \int_{-\frac{t}{2}}^{\frac{t}{2}} \begin{bmatrix} \sigma_x \\ \sigma_y \\ \tau_s \end{bmatrix} z \, dz
$$

Now we can consider a multilayer laminate and find the total force and moment components

on it, by summing them layer by layer.

$$
\begin{bmatrix} N_x \\ N_y \\ N_s \end{bmatrix} = \sum_{k=1}^{n} \int_{z_{k-1}}^{z_k} \begin{bmatrix} \sigma_x \\ \sigma_y \\ \tau_s \end{bmatrix} dz
$$

$$
\begin{bmatrix} M_x \\ M_y \\ M_s \end{bmatrix} = \sum_{k=1}^{n} \int_{z_{k-1}}^{z_k} \begin{bmatrix} \sigma_x \\ \sigma_y \\ \tau_s \end{bmatrix} z \, dz
$$

The limits of the integration represent the upper and lower surfaces of a layer k, and there

can be an arbitrary number layers in the summation.

The equations for stress in terms of strain and reduced stiffness can be substituted to obtain:

$$
\begin{bmatrix} N_x \\ N_y \\ N_s \end{bmatrix} = \sum_{k=1}^{n} \left\{ \begin{bmatrix} Q_{xx} & Q_{xy} & 0 \\ Q_{yx} & Q_{yy} & 0 \\ 0 & 0 & Q_{ss} \end{bmatrix} \begin{bmatrix} \varepsilon_x^0 \\ \varepsilon_y^0 \\ \gamma_s^0 \end{bmatrix} \int_{z_{k-1}}^{z_k} dz + \begin{bmatrix} Q_{xx} & Q_{xy} & 0 \\ Q_{yx} & Q_{yy} & 0 \\ 0 & 0 & Q_{ss} \end{bmatrix} \begin{bmatrix} \kappa_x \\ \kappa_y \\ \kappa_s \end{bmatrix} \int_{z_{k-1}}^{z_k} z \, dz \right\}
$$

$$
\begin{bmatrix} M_x \\ M_y \\ M_s \end{bmatrix} = \sum_{k=1}^{n} \left\{ \begin{bmatrix} Q_{xx} & Q_{xy} & 0 \\ Q_{yx} & Q_{yy} & 0 \\ 0 & 0 & Q_{ss} \end{bmatrix} \begin{bmatrix} \varepsilon_x^0 \\ \varepsilon_y^0 \\ \gamma_s^0 \end{bmatrix} \int_{z_{k-1}}^{z_k} z \, dz + \begin{bmatrix} Q_{xx} & Q_{xy} & 0 \\ Q_{yx} & Q_{yy} & 0 \\ 0 & 0 & Q_{ss} \end{bmatrix} \begin{bmatrix} \kappa_x \\ \kappa_y \\ \kappa_s \end{bmatrix} \int_{z_{k-1}}^{z_k} z^2 \, dz \right\}
$$

These equations can be rewritten as:

$$[N]_{xy} = [A]_{xy}[\varepsilon^0]_{xy} + [B]_{xy}[\kappa]_{xy}$$

$$[M]_{xy} = [B]_{xy}[\varepsilon^0]_{xy} + [D]_{xy}[\kappa]_{xy}$$

The equations have been organized in terms of four matrices, [A], [B] and [D]. These are called

the laminate stiffness matrices and represent specific properties of a laminate. [A] is the

extensional stiffness matrix and relates in plane loads to strains. [B] is *coupling stiffness* which

relates in plane loads to curvatures and moments. [D] represents *bending stiffness* for the

laminate, and relates moments to curvatures. These matrices are also symmetric. The formulas

for these matrices are :

$$[A]_{ij} = \sum_{k=1}^{n} Q_{ij}^k (z_k - z_{k-1})$$

$$[B]_{ij} = \frac{1}{2}\sum_{k=1}^{n} Q_{ij}^k (z_k^2 - z_{k-1}^2)$$

$$[D]_{ij} = \frac{1}{3}\sum_{k=1}^{n} Q_{ij}^k (z_k^3 - z_{k-1}^3)$$

The force and moment equations can be combined into one general equation in terms of the

[A],[B], [D] matrices, strains and curvatures, which results in:

$$
\begin{bmatrix} N_x \\ N_y \\ N_s \\ M_x \\ M_y \\ M_s \end{bmatrix} =
\begin{bmatrix}
A_{xx} & A_{xy} & A_{xs} & B_{xx} & B_{xy} & B_{xs} \\
A_{yx} & A_{yy} & A_{ys} & B_{xy} & B_{yy} & B_{ys} \\
A_{sx} & A_{sy} & A_{ss} & B_{xs} & B_{sy} & B_{ss} \\
B_{xx} & B_{xy} & B_{xs} & D_{xx} & D_{xy} & D_{xs} \\
B_{yx} & B_{yy} & B_{yy} & D_{yx} & D_{yy} & D_{ys} \\
B_{sx} & B_{sy} & B_{ss} & D_{sx} & D_{sy} & D_{ss}
\end{bmatrix}
\begin{bmatrix} \varepsilon_x^0 \\ \varepsilon_y^0 \\ \gamma_s^0 \\ \kappa_x \\ \kappa_y \\ \kappa_s \end{bmatrix}
$$

The formulas for the calculation of stiffness matrices [A] and [D] were found in the Chen-Tsai journal article [2]. Matrix [B] is zero because the laminate is symmetric [3]. The formula for the [A] matrix is as follows:

$$[A^{rib}] = \begin{bmatrix} \frac{E_x A_0}{d_0} + 2\frac{E_x A_\theta}{d_\theta}m^4 & 2\frac{E_x A_\theta}{d_\theta}m^2 n^2 & 0 \\ 2\frac{E_x A_\theta}{d_\theta}m^2 n^2 & \frac{E_x A_{90}}{d_{90}} + 2\frac{E_x A_\theta}{d_\theta}n^4 & 0 \\ 0 & 0 & 2\frac{E_x A_\theta}{d_\theta}m^2 n^2 \end{bmatrix} \quad \begin{array}{l} m = \cos(\theta) \\ n = \sin(\theta) \end{array}$$

Ex is the Young's modulus, $A0$, $A90$ and $A\theta$ are the cross sectional areas of the vertical, horizontal and angled ribs respectively. Similarly, $d0$, $d90$ and $d\theta$ are the lengths of the vertical, horizontal and angled ribs respectively.

Composite matrix [D] can be calculated as follows:

$$[D^{rib}] = \begin{bmatrix} D_{11}^{rib} & D_{12}^{rib} & 0 \\ D_{21}^{rib} & D_{22}^{rib} & 0 \\ 0 & 0 & D_{66}^{rib} \end{bmatrix}$$

$$D_{11}^{rib} = \frac{E_x I_0}{d_0} + 2\frac{E_x I_\theta}{d_\theta}m^4 + 2\frac{E_s J_\theta}{d_\theta}m^2 n^2$$

$$D_{22}^{rib} = \frac{E_x I_{90}}{d_{90}} + 2\frac{E_x I_\theta}{d_\theta}n^4 + 2\frac{E_x J_\theta}{d_\theta}m^2 n^2$$

$$D_{12}^{rib} = D_{21}^{rib} = 2\frac{E_x I_\theta}{d_\theta}m^2 n^2 - 2\frac{E_s J_\theta}{d_\theta}m^2 n^2$$

$$D_{66}^{rib} = 2\frac{E_x I_\theta}{d_\theta}m^2 n^2 + \frac{E_s J_0}{4d_0} + \frac{E_s J_{90}}{4d_{90}} + \frac{E_s J_\theta}{2d_\theta}(m^2 - n^2)$$

2.5)   Finite Element Analysis of Stiffened Plates

Hypermesh and Optistruct were used for the FEM analysis, and both tools are part of the Altair HyperWorks software suite. HyperWorks was used because it enables easy selection of many different types of mesh elements, which reduces modeling and analysis time. Solid elements were inappropriate for simulating the geometry being analyzed.

One dimensional rod elements were used to simulate the carbon segments on the top and bottom of the grid. Using 1D elements reduced run time, set up time and were more suited to simulating the behavior of the carbon segments. One dimensional elements are used when a single dimension of the geometry being analyzed is much larger than the other two [5 p.170]. The carbon segment cross section width was 1mm and the thickness was 0.125mm. However, the carbon fibers could be up to 254mm long. Therefore one dimensional elements were appropriate for the simulation. Hypermesh allows easy use of 1D elements, where the cross sectional area of the rod segments were set to be equal to the cross sectional area of the carbon, which was equal to 0.125mm^2.

Furthermore, rod elements were used over other types of one dimensional elements (such as bar or beam elements) because rod elements were judged to more appropriately simulated the behavior of the real carbon segments. Rod elements resist loads in tension, compression and torsion [5, p. 171]. However, the CROD elements were used for the analysis, and they support tension and compression only [5. p.182]. Bending loads ultimately resolve into compression and tension, and since the carbon is placed where it is most effective in resisting bending loads, rod elements were used.

Two dimensional shell elements are used when two dimensions (length and width) are much larger than the third dimension (thickness). The skin thickness can be assigned as a property of

the shell elements, and can be quickly changed when needed, without having to remodel the geometry. The wall thickness of the nylon ribs was 0.125mm, while the roof and floor layers were 0.5mm thick, but the height of the ribs was 12.7mm. The ribs are 254mm long. Therefore, shell elements were appropriate for modelling the nylon segments of the grids. As with 1D rod elements, 2D shell elements can significantly reduce the modeling time, and simulation run time for analysis when used correctly.

3) Methodology

To manufacture parts with the Markforged Mark Two, they were first modeled using SolidWorks. In order to successfully print composite grids, it was very important to be ensure that the ribs were thick enough for carbon to be embedded in them. Then the parts were saved as STL files and uploaded to the cloud based Eiger software. Specific setting had to be used in Eiger to successfully print parts with thin nylon skin and to have carbon in the correct layers and orientation. In particular, each layer of the print that was to have carbon fiber needed to have customized settings, rather than relying on the automatic settings in Eiger.

To calculate the stiffness matrices of the laminate stiffener grid, the moments of inertia of each rib must be calculated. The rib dimensions, moments of inertia and material properties are used to calculate the stiffness matrices [A] and [D], which can then be used to calculate bending stiffness. Once bending stiffness has been obtained, deflection can be calculated using Euler beam bending equations. Deflection was calculated for cantilevered and simply supported loadings, with a 9.81N applied force.

Altair Optistruct was used to computationally predict deflection, using the finite element method. Since nylon layers on the ribs are very thin, they were simulated using two dimensional shell elements. Since the carbon fibers are only effective at resisting bending loads, one dimensional rod elements were used to simulate the carbon layers.

For the cantilevered beam experiment, the grid was clamped down on one end to a table and a fixture with a hook was clamped onto free end. Then, masses were hung from the hook, to load the grid in bending. The progressively larger masses were loaded onto the hook, up to a maximum mass of 1000 grams (1kg) which resulted in a 9.81N force being applied to the end of the grid.

3.1) Manufacturing

The Markforged Mark two printer was used to print the stiffener grids. This particular printer was originally a Mark One, which was upgraded to a Mark Two. There are two separate heads that extrude Nylon and Carbon fiber filament. The Mark Two print Nylon parts via the Finite Deposition Modeling process and then embeds carbon fiber into the nylon parts via the heated carbon extrusion nozzle (the CFF process). Thus, the Markforged printer can produce layers of continuous carbon fiber with a nylon matrix.

The Markforged continuous fiber printing process offers great potential for printing light and stiff parts. Fiber orientation can be used to tailor stiffness properties. Nylon infill can be greatly reduced since the carbon fiber can be positioned to provide most of the stiffness.

However, the Mark Two printer owned by UTA demonstrated many different kinds of print failures, both due to hardware and software issues. Markforged requires the use of a cloud based slicing software to set up the prints, and the software is very limited regarding the degree of control available to the user.

The cloud based slicing software is named Eiger, and can be used ONLY with the Google Chrome browser, which is the first limitation encountered by a potential user. Although Chrome is free and easy to install, often there are university computers which do not have chrome installed due to school policy/security concerns.

The grids were initially modelled in SolidWorks, which is relatively simple and straightforward. The grid was sketched on a plane in a manner such that there were repetitive orthotropic cells. Then the lines were offset bilaterally 3.9 mm and the sketch was trimmed, to allow the grid to be extruded with a single sketch. The critical measurements is the width of the ribs. The ribs must have a minimum width in order to be able to put carbon in them.

The minimum width was determined to be 3.9mm based on trial and error over many test prints on smaller parts. Sometimes, it was possible to reduce the rib width to 3.7 mm but that only worked for simpler parts (single ribs for example, with no grids). However, the results were very inconsistent with any width less than 3.9mm, thus it is recommended to be the minimum width for printing stiffening grids with the Markforged Mark Two.
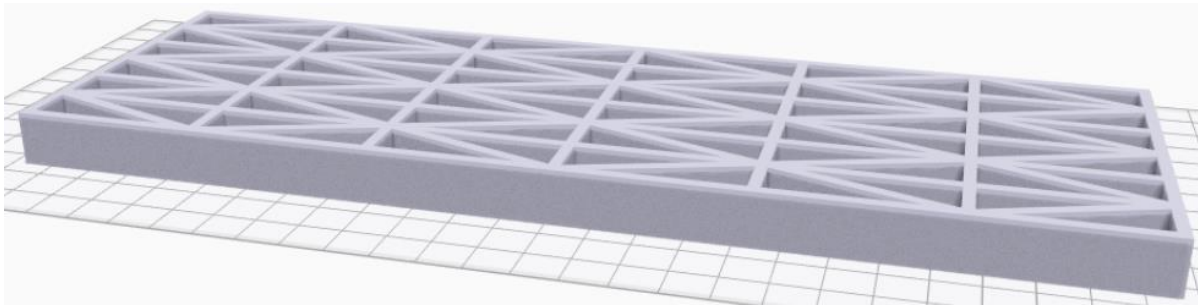
Figure 14 Orthotropic Grid Model, viewed in Eiger

The model is saved as an STL file and then uploaded to Eiger. When the Solidworks part is exported to STL, it should be ensured that the exported units are correct (check if it is exported as imperial or metric). The part is then oriented such that it is flat on the plate and centered. Furthermore, it must be ensured that the units are set correctly in Eiger, otherwise the part will be far too large or small.

Eiger slices the part automatically. However, in order to ensure correct fiber placement, certain slicing setting must be applied and then individual layers must be modified. Eiger has three subsections under which various settings are grouped, which affect the automated slicing. They are labelled 'General', 'Settings' and 'Infill'.

Under General, 'Reinforcement Material' must be selected to be Carbon fiber. For 'Settings', the 'Layer Height' could not be adjusted and was fixed at 0.125 mm. However, the 'Original Units' were set to Metric, 'Use Supports' and 'Expand Thin Features' were turned off, but 'Brim' was turned on to reduce the tendency of parts to curl. Under 'Infill', Fill Pattern was selected to be

Rectangular Fill, Fill Density was set to 5%, Roof & Floor layer was set to three, and there was only one Wall Layer.
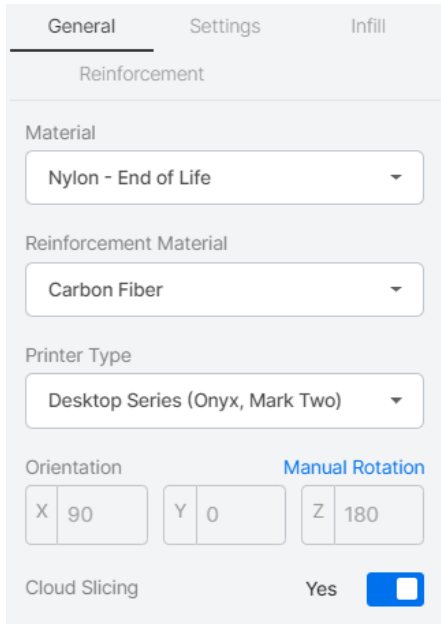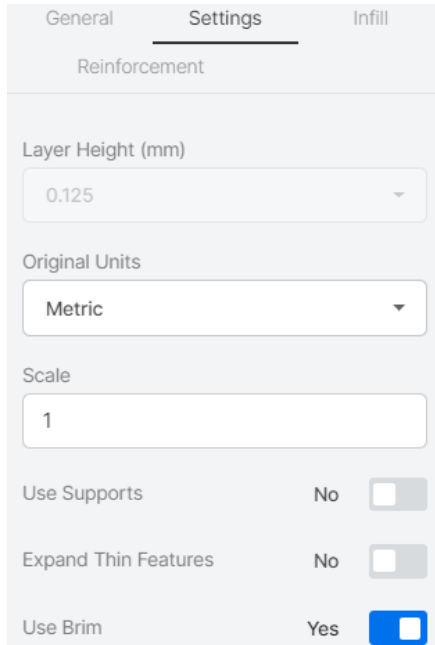

Figure 15 General Options on Eiger
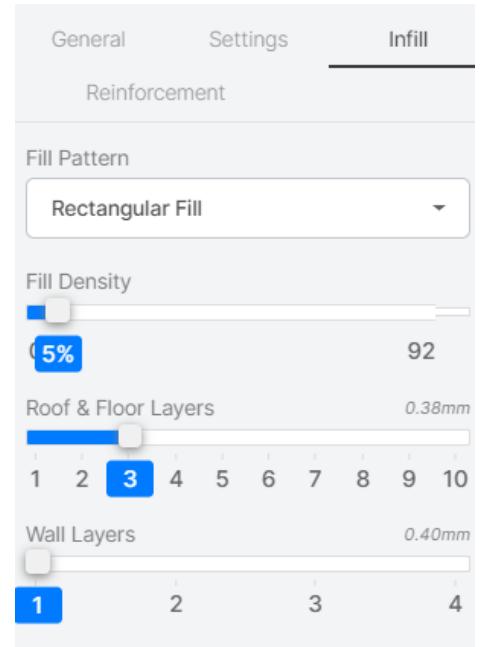
Figure 17 Settings Options on Eiger

Figure 16 Infill Options on Eiger

It should be noted however, these settings do not agree with those recommended by Markforged. The recommended settings are four layers for the roof and floor, and at least two wall layers. Furthermore, Eiger shows that the thickness of a single wall layer is 0.4mm, however measuring the wall layers of printed parts showed they were 0.65mm thick.

To develop a process for printing grids with carbon on the top and bottom surfaces of stiffening ribs, an iterative process was used, where simple shapes were printed first and then more complex grids were modelled and sliced. Along the way there, were many failed parts and errors in printing, some of which could not be corrected. However, even with the errors it was possible to print the desired beam, constructed out of orthotropic grid cells.

The first step was to print a single orthotropic grid cell, with horizontal, vertical and angled ribs. It was discovered that it was not possible to instruct the software to print the carbon along the

correct direction, unless multiple layers of carbon were printed, witch the fiber oriented along particular directions. For example, it was found that it was possible to print horizontal and vertical fibers, but not angled fibers on the same layer.
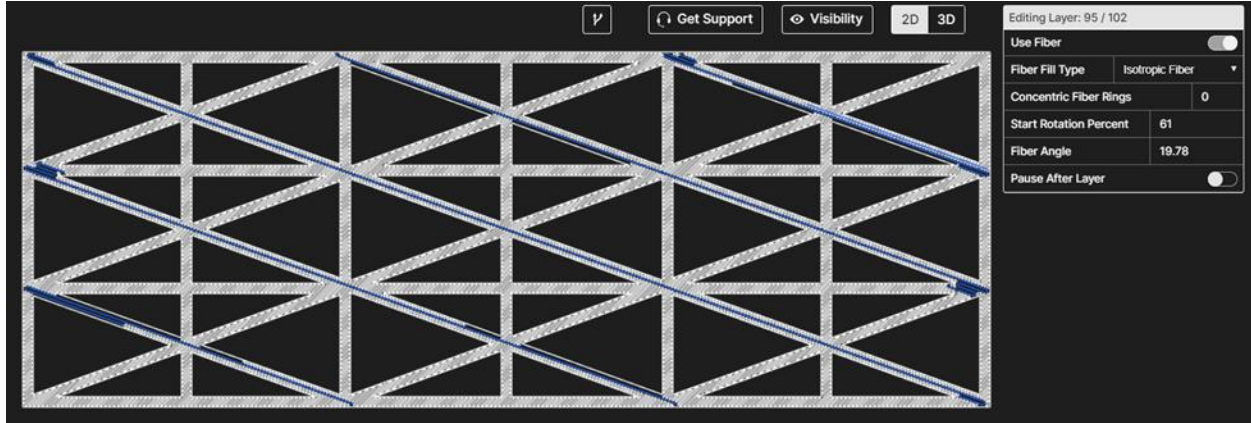

Figure 18 Layer with 19.76 degree fiber angle
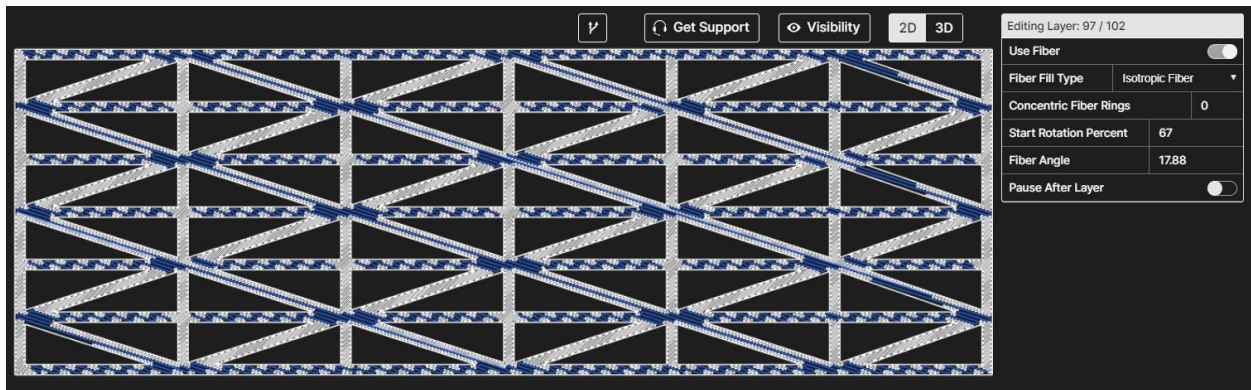
Figure 19 Orthotropic Grid with wavy fibers

To print fibers along the angled ribs, certain settings had to be selecting within the Eiger slicing software. For a given layer, the 'Use Fiber' option must be select and the 'Fiber Fill Type' must be set to 'Isotropic Fiber' (although the fiber layout is not actually going to result in isotropy at all, this is the option that needs to be used). There must be no 'Concentric Fiber Rings' (set to zero) and 'Start Rotation Percent' seems to be irrelevant and can be at any arbitrary value that the software picks. The key setting however, is 'Fiber Angle'.

'Fiber Angle' must be set to the angle of the ribs. Otherwise there is a chance that the slanted ribs will not have any fiber placed in them. Furthermore, it was found from trial and error that the angle must be accurate to the second decimal place (0.01 degrees). To put down fiber along the ribs angled in the opposite direction, the next layer of carbon should be sliced using the exact same settings, but with the negative value of the required angle.

However, as complexity of the geometry increased, the errors in fiber placement also propagated. When the final geometry was sliced for printing, there were many errors with carbon fiber layout that could not be removed by adjusting settings within Eiger. In particular, with the final part, there were layers with wavy filaments laid down in places where there should not have been any fiber at all, especially when the layer had been set to have fibers along the angled ribs.

3.2) Analytical Deflection Prediction

All the ribs have the same cross section and are hollow. The Markforged Mark Two printer can be instructed to print with very low infill percentage. For the orthotropic grids, 5% rectangular infill was used. Thus, the ribs can be treated as small box beam. Furthermore, the beam can be divided into separate nylon and carbon segments, which allows for moment of inertia to be calculated for them separately.
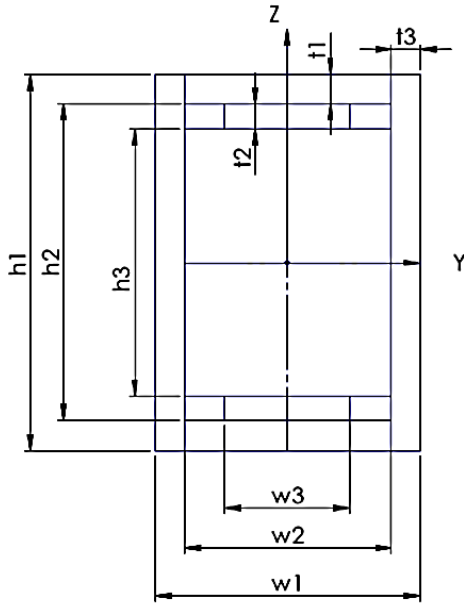

Figure 20 Rib dimensions diagram

Table 1 Height and Width Values

height and width	(mm)
h1	12.7
h2	11.95
h3	11.7
w1	2.69
w2	1.39
w3	1

Table 2 Thickness Values

skin thickness	(mm)
t1	0.375
t2	0.125
t3	0.65

The outer dimensions of the rib are *h1* and *w1*, which respectively represent the height and width. The dimensions *h2* and *w2* are the height of the composite layers of the rib. The dimensions of the central cavity are *h3* and *w3*. Thickness of the top layer of nylon is *t1* and the carbon layer is *t2*. The thickness of the skin on the sides of the rib is *t3*. Also, since the cross section is a rectangle, the centroid is located in the center. The centroid is chosen to be the origin of a co-ordinate system.

The rib cross sectional area is divided into small rectangular segments, that are labeled alphabetically from A to J. Segments A to H are nylon. Segments I and J and are carbon. Since the cross section was divided into rectangles, the centroid of each individual segment was simply the

location of the center of each rectangle. The y coordinates of each centroid was labeled yA to yJ, in alphabetical order. In the same way, the z coordinates of each centroid was labeled zA to zj.
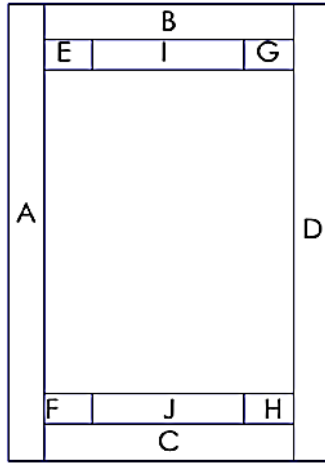

Figure 21 Rectangular Segments

Table 3 Segment Labels and Material

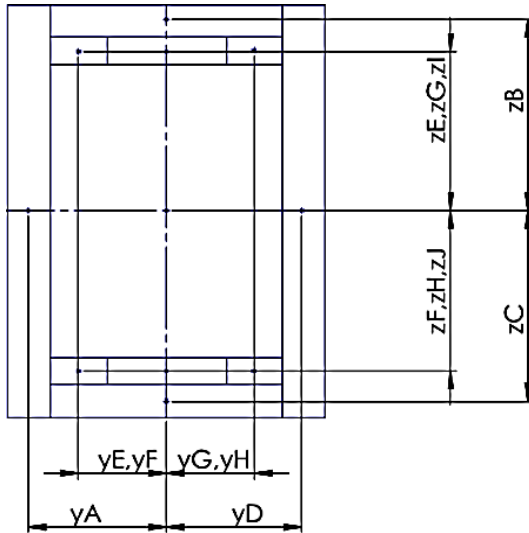| segment	material
A	nylon
B	nylon
C	nylon
D	nylon
E	nylon
F	nylon
G	nylon
H	nylon
I	carbon
J	carbon

Figure 22 segment centroid co-ordinates

Table 4 segment centroid coordinates

centroid y coordinate	dimension (mm)	centroid z coordinate	dimension (mm)
yA	-1.02	zA	0
yB	0	zB	6.16
yC	0	zC	-6.16
yD	0.598	zD	5.91
yE	-0.598	zE	-5.91
yF	-0.598	zF	5.91
yG	0.598	zG	-5.91
yH	0.598	zH	5.91
yI	0	zI	-5.91
yJ	0	zJ	5.91

The values of the centroid coordinates were calculated and then tabulated. Calculation of the centroid coordinates was performed initially by hand, then implemented with a Python script. The moment of inertia of each segment was calculated and in order to do that, the height and width of each segment were determined. The heights were labeled hA to hJ. The width were labeled hA to hJ. The values were again, calculated both by hand and then with a python script.
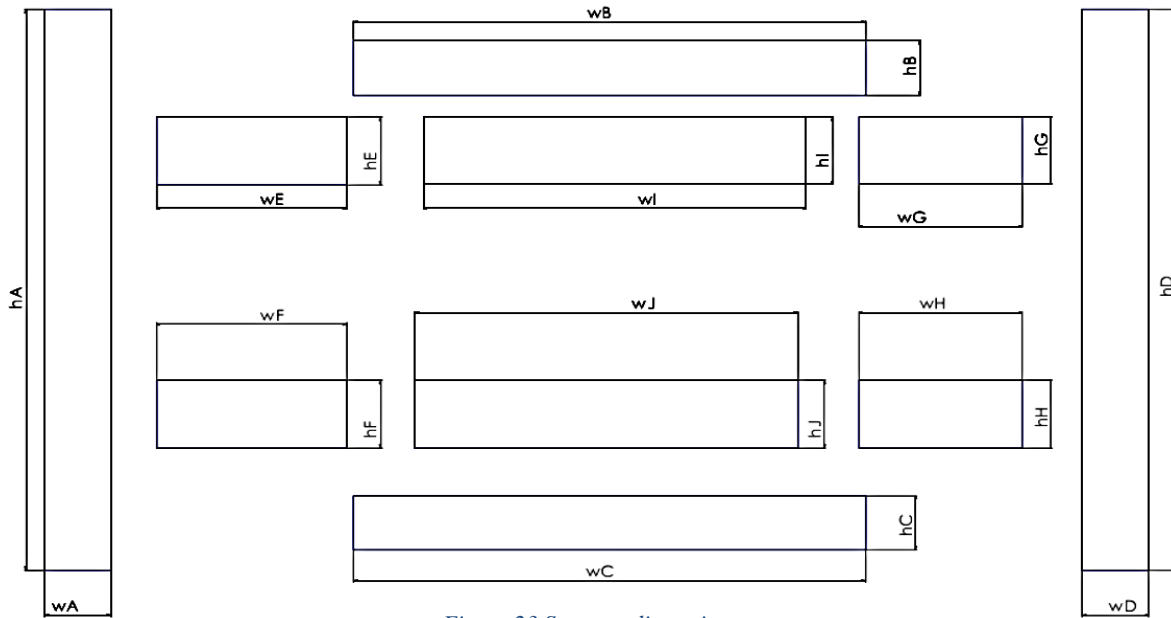
Figure 23 Segment dimensions

Table 5 Segment heights and widths

segment height	dimension(mm)	segment width	dimension(mm)
hA	12.7	wA	0.65
hB	0.375	wB	1.39
hC	0.375	wC	1.39
hD	12.7	wD	0.65
hE	0.125	wE	0.195
hF	0.125	wF	0.195
hG	0.125	wG	0.195
hH	0.125	wH	0.195
hI	0.125	wI	1
hJ	0.125	wJ	1

The ribs were arranged in an orthotropic grid, to construct a 10.00in by 3.33in rectangle. The grid was constructed of nine orthotropic grid elements that are repeated until the whole rectangle was formed.
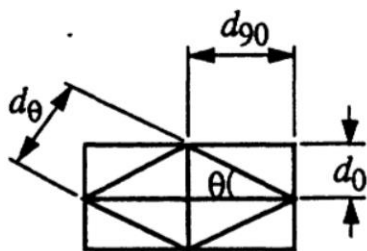

Figure 24 Orthotropic Grid Unit

Table 6 Rib length dimensions

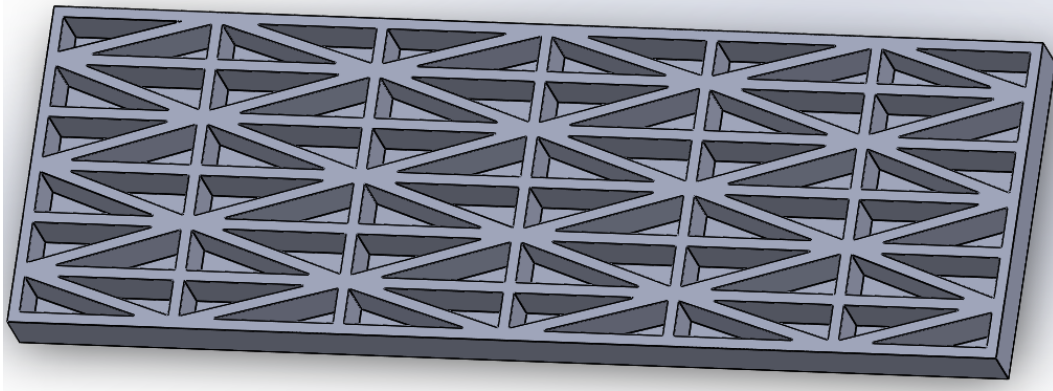| rib legths	dimension
d0	12.55(mm)
d90	40.89(mm)
dθ	42.77(mm)
θ	17.06 (degree)

Figure 25 Orthotropic Grid Test Piece

A larger test piece should be constructed in the future, however there were serious constraints in the 3d printing process. The large pieces were suffering curling and shrinkage issues, as well as burning and delamination between layers.

To attempt to predict the behavior of the ribs analytically, the moment of inertia of the rib needed to be calculated using the basic formula for a square cross section, and by using parallel axis theorem. Since there are equivalent layers of carbon on the top and bottom surfaces, the beam can be thought of as a symmetric laminate, thereby simplifying the calculation of composite stiffness matrices. Also, the method for calculating the compliance matrices for a composite orthotropic grid were available in prior work conducted by Tsai Chen
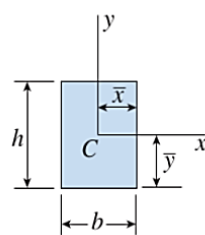
Rectangle (Origin of axes at centroid)

$$A = bh \qquad \bar{x} = \frac{b}{2} \qquad \bar{y} = \frac{h}{2}$$

$$I_x = \frac{bh^3}{12} \qquad I_y = \frac{hb^3}{12} \qquad I_{xy} = 0 \qquad I_P = \frac{bh}{12}(h^2 + b^2)$$

Figure 26 2nd moments of inertia of rectangle [1]

Also, since the rib cross section was divided into several segments, the moment of inertia can also be calculated separately for carbon and nylon segments, which can give be used to separately calculate the stiffness of the carbon and nylon segments. This can help with understanding the

43

contribution of nylon to the structural performance of the rib. The formula for rectangular cross sections was found in the Gere solid mechanics book [1, p.966].

Parallel axis theorem was then used to calculate the moment of inertia about the neutral axis of the rib. The theorem and the formula were also found in the Gere book [1, p. 912]. Second moment of inertia was calculated about both the z and y axes. This because torsional stiffness would need to be considered.

$$I_x = I_{xc} + Ad^2$$

Then, the laminate stiffness matrices had to be calculated, the [A], [B] and [D] matrices. The [A] matrix relates in plane stress to in plane strain and it is called the extensional stiffness matrix. The [B] matrix relates in plane stress to curvature, and in plane moments to plane strain, and it is called the coupling stiffness matrix. Moments are related to curvatures with the [D] matrix, the bending stiffness matrix. [3, p.165]

In order to find utilize the formulas, a number of geometric properties must be calculated, especially moment of inertia and cross sectional area. The cross sectional areas of the ribs are constant. Thus *Aθ*, *A90* and *A0* (the areas of angled, horizontal and vertical ribs) are all equal to 34.163mm^2. The moments of inertia were calculated with a script and the results are tabulated.

Table 7 Inertia Table

y inertia	value (m4)	z inertia	value (m4)
IAy	1.11E-10	IAz	8.88E-12
IBy	1.98E-11	IBz	8.39E-14
ICy	1.98E-11	ICz	8.39E-14
IDy	1.11E-10	IDz	8.88E-12
IEy	8.52E-13	IEz	8.78E-15
IFy	8.52E-13	IFz	8.78E-15
IGy	8.52E-13	IGz	8.78E-15
IHy	8.52E-13	IHz	8.78E-15
IIy	4.37E-12	IIz	1.04E-14
IJy	4.37E-12	IJz	1.04E-14
Iy Total	2.74E-10	Iz Total	1.80E-11

Polar moments of inertia can be calculated from Iy Total and Iz Total with the formula:

$$J = I_x + I_y$$

The reference book uses the symbol Ip for polar moment, but the Tsai article uses J. For the rest of this document, J will be used for polar moment of inertia.

From the PHD dissertation of UTA student GIANFRANCO RIOS [4, p.29], a formula was found for calculating the bending stiffness of the test piece. Consider a beam with a wide cross section (width is much larger than thickness), with a width of *w*.
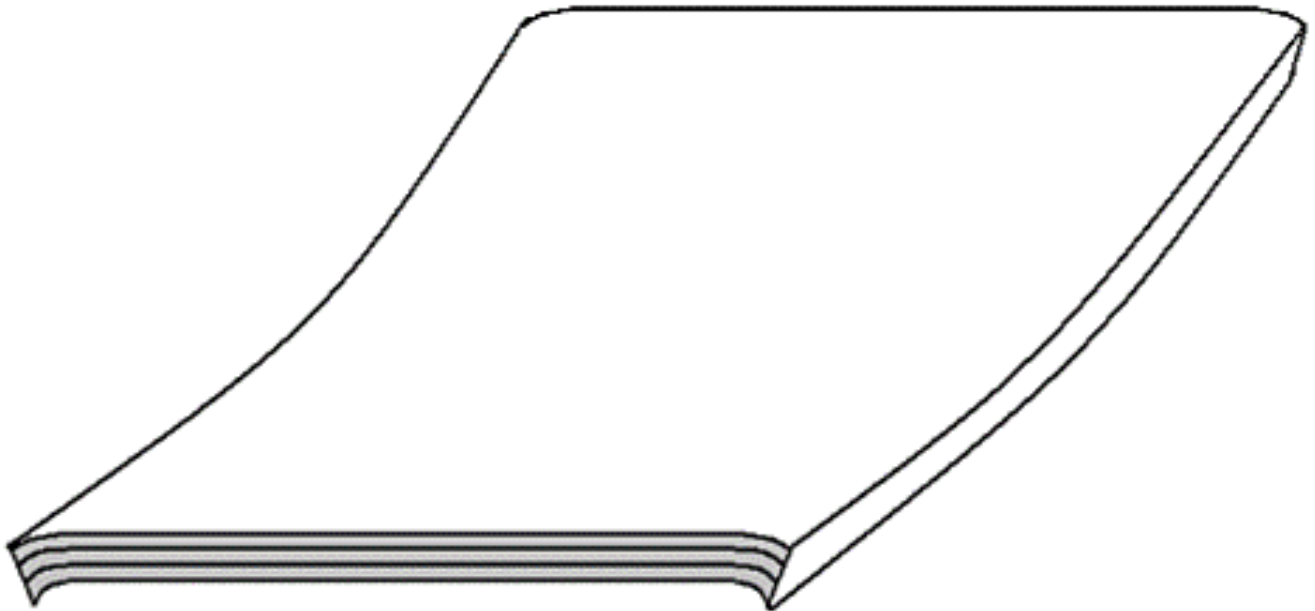
Figure 27 Wide beam with deformed cross section [4]

The equation D_x^{wide} refers to bending stiffness of the wide beam:

$$D_x^{wide} = w \left(D_{11} - \frac{B_{11}^2}{A_{11}} \right)$$

For a symmetric laminate, [B] is zero, and the equation reduces to $D_x^{wide} = w D_{11}$, where *w* represents the width of a wide beam. This means there is an extremely simple formula for calculation of bending stiffness for composite grids with symmetric laminates.
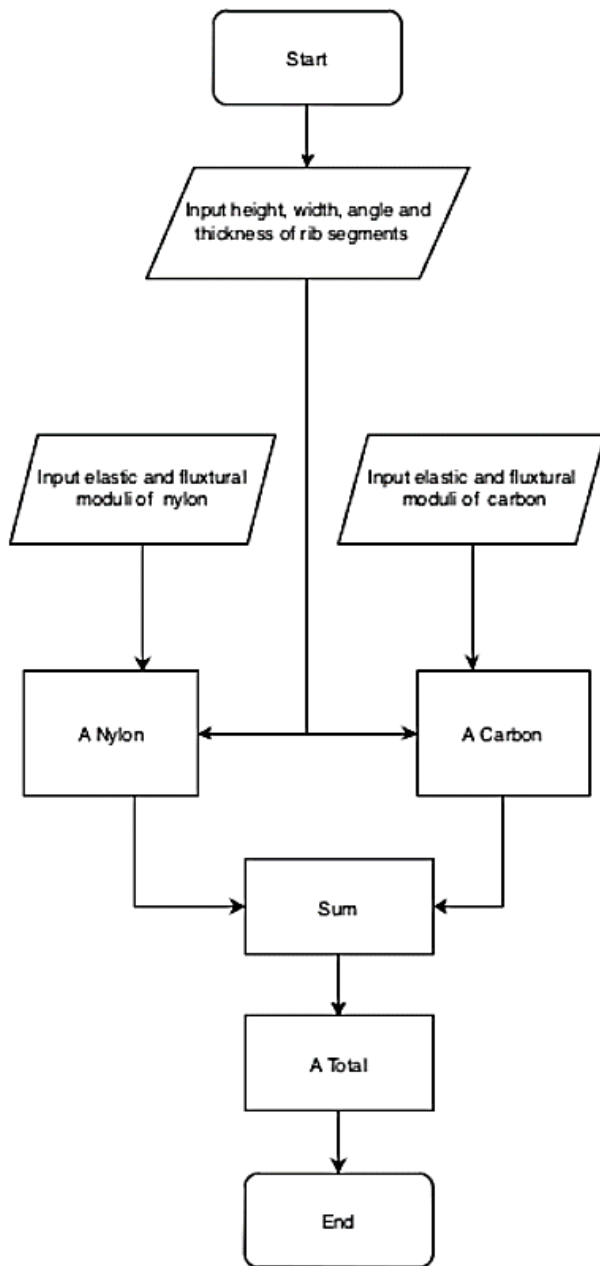
Figure 28 [A] Matrix Calculation Flowchart

To explain the logic of the calculations, several flow charts were drawn. Even though a single program was used, it was easier to draw three flow charts to explain the calculations. One flow chart was drawn for the [A] Matrix, another for the [D] matrix and a final flow diagram which illustrates how the [D] matrix is used to calculate bending stiffness. After obtaining bending stiffness, it is simple to use the deflection formulas to obtain deflections for an applied load. These calculations can then be compared to FEM analysis.

To calculate the [A] matrix with a script, the rib dimensions (height, width, thicknesses of skin layers and angle of the ribs) need to be in the input. Other inputs needed are elastic and flexural moduli of nylon and carbon. The matrix can be calculated using the formula from the Tsai-Hill paper, which was stated in the background section.

The extensional stiffness matrices for Carbon and Nylon segments were to be calculated separately, then they need to be added together to get [A] Total, which is the needed extensional stiffness matrix.
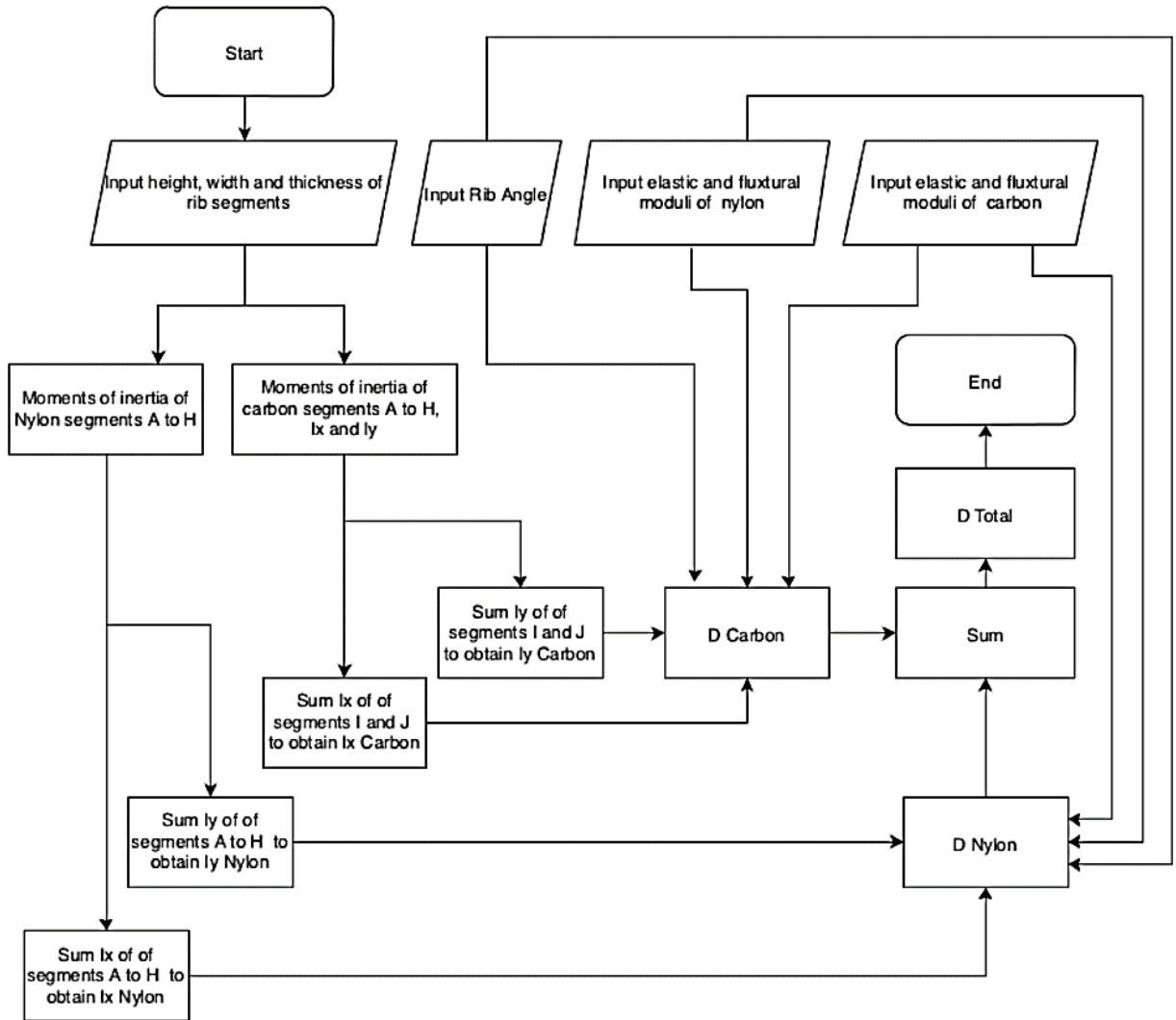
46

Figure 29 [D] Matrix Calculation Flowchart

The [A] matrix is not dependent upon moment of inertia, which makes it much simpler to calculate compared to the [D] matrix. However, the extensional stiffness matrix was not utilized for calculating the bending stiffness because a very simple formula was used. It was included in the calculations though, because there is potential for predicting other properties, or to use more refined analytical methods for calculating stiffness and deflection. In particular, axial loading and buckling behavior would be worth investigating.

To calculate the bending stiffness matrix [D], the moments of inertia of each segment of the rib cross section must be calculated separately. Thus, the dimensions of the ribs and the segments from A to J must be inputted. Second moment of inertia for the carbon and nylon segments need to calculated along both the x and y axes.
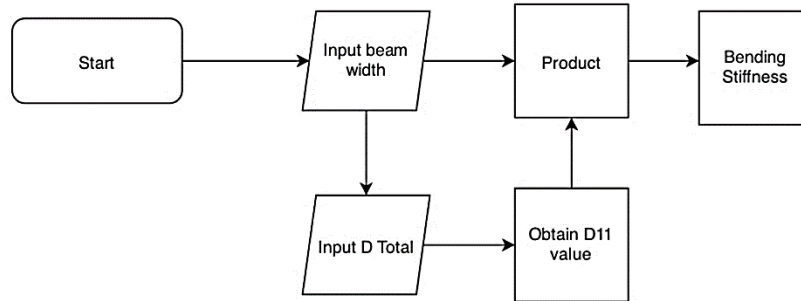

Figure 30Bending Stiffness Calculation Flowchart

Rib angle, elastic and flexural moduli of both nylon and carbon must also be inputted, and then they can be used along with the moments of inertia to calculate [D] Carbon and [D] Nylon separately. Summing them results in [D] Total, which is the laminate bending stiffness for the whole grid.

Once the bending stiffness matrix has been calculated, bending stiffness can be found. Input the beam width and the already calculated D Total matrix, then multiply D11 with the beam width. The product is the bending stiffness. The bending stiffness can be used in beam deflection formulas to predict maximum deflection.
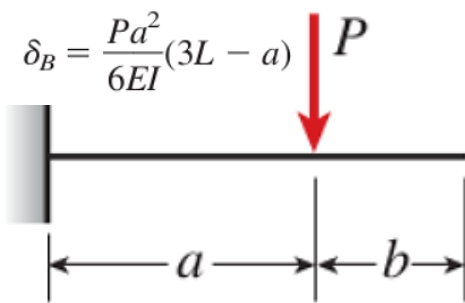
$$\delta_B = \frac{Pa^2}{6EI}(3L - a)$$

Figure 32 Cantilever beam diagram and deflection formula [1]

$$\delta_C = \delta_{max} = \frac{PL^3}{48EI}$$

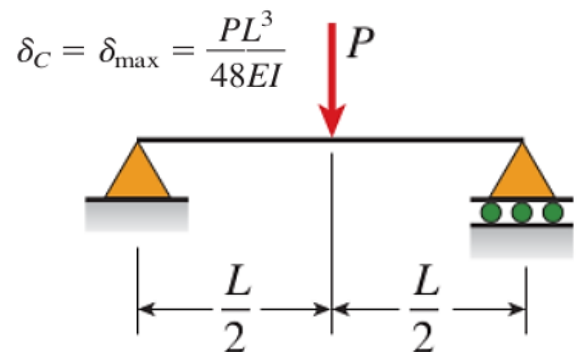*Figure 31 Simply supported beam diagram and formula [1]*

For the cantilevered beam, length L was 8.5 inches and length a was 7.750 inches. In metric units, L was 215.9mm and a was 196.85mm. Load P was 9.81 N. For the simply supported beam, L was 7 inches, or 177.8mm. P was again 9.81 N. In both deflection formulas, the product EI was replaced with the bending stiffness D_x^{wide}.

3.3) Optistruct deflection prediction

The beam was analysed with Optistruct for two load cases. A cantlivered beam loading and a simply supported beam loading. The deflection for each case was to be analysied, for a 9.81N load applied onto the beam. The beam was modeled using 2d surfaces rather than solid elements, due to the walls of the ribs consisting of very thin layers of nylon. The carbon segments on the top and bottom of the ribs were modelled as 1 dimensional rods.

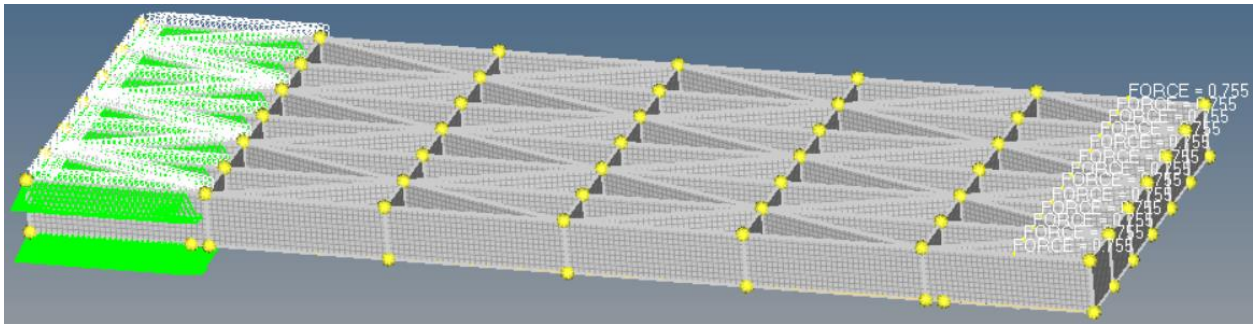*Figure 33 Cantilevered beam model*

The cantilevered beam was supported in a manner that simulates it being clamped down with an aluminum bar, with a 1.5 inch width (38.1 mm). The load was placed at the centroid of a rectangular distributed load, that would be placed on the beam by a 1.5in (38.1mm) inch wide wooden block, with a 9.81 N weight on it.
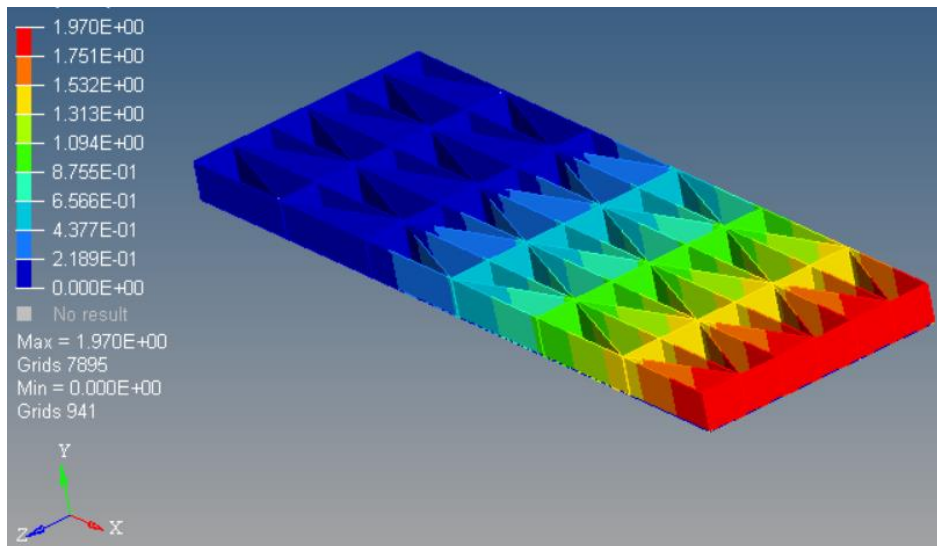

Figure 34 Cantilevered beam deflection plot

The simply supported beam analysis placed supports that were 7 inches (177.8 mm) apart. This was done because the expirimental test fixture that was supposed to be used for the physical testing, was only seven inches wide, even though a ten inch fixture would have been preferable. A force of 9.81 N was applied to the middle of the beam, divided between seven nodes.

Figure 35 Simply supported beam

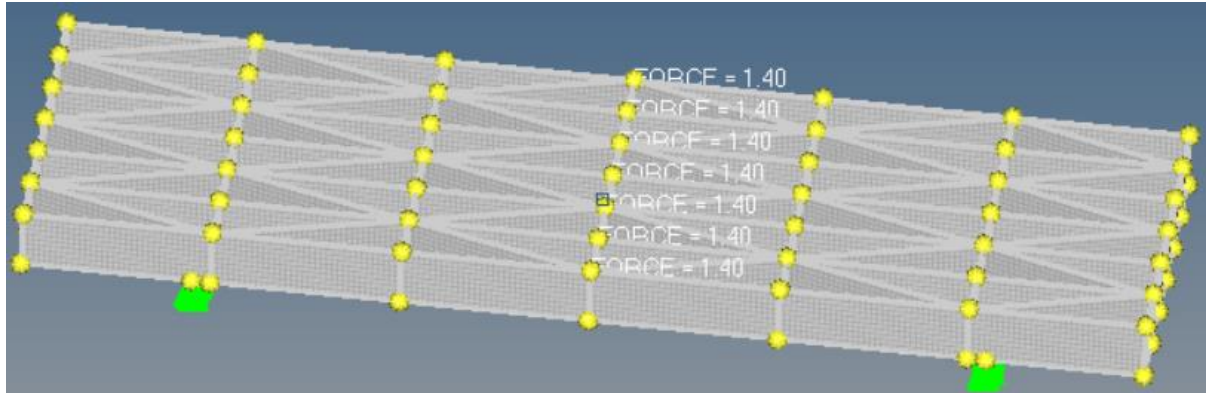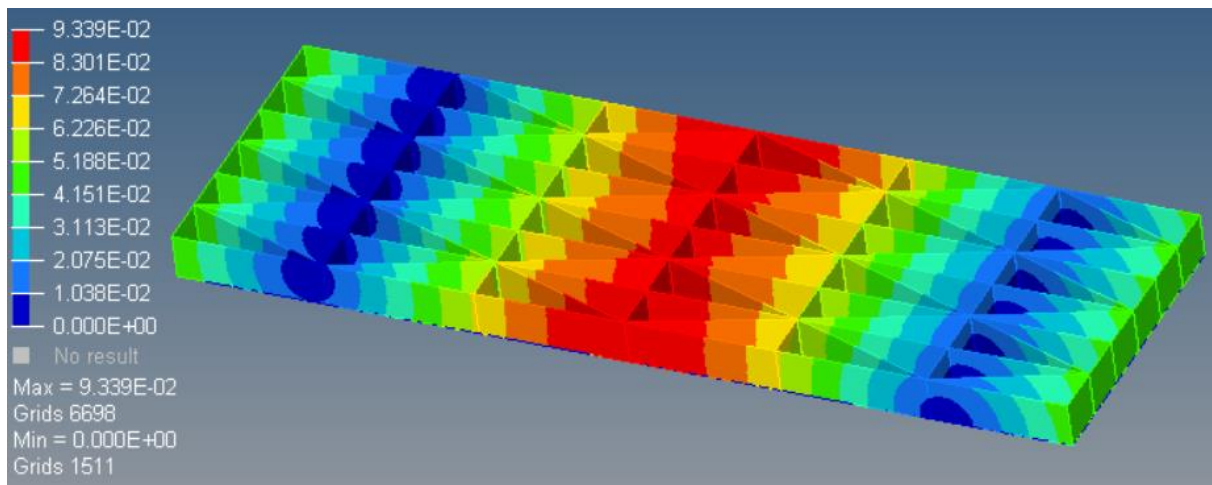*Figure 36 Simply Supported beam deflection*

After comparing the results of the FEM analysis with the analytical and experimental results, it was discovered that the FEA results did not agree with the other ones. The sources of this error could not be discovered in the time that was available, however the most likely source of error are the carbon material properties and the one dimensional elements.

3.4) Experimental method

To test the grid in cantilevered loading, the apparatus in the figure below was used (due to lack of access to more sophisticated apparatus). The dial indicator used to measure the displacements was graduated in thousandths of an inch (0.001"). Therefore, the displacements had to be converted to millimeters after being measured. The test piece was clamped onto a table using a steel C clamp, with an aluminum bar being used to distribute the clamping forces over the whole width of the beam.
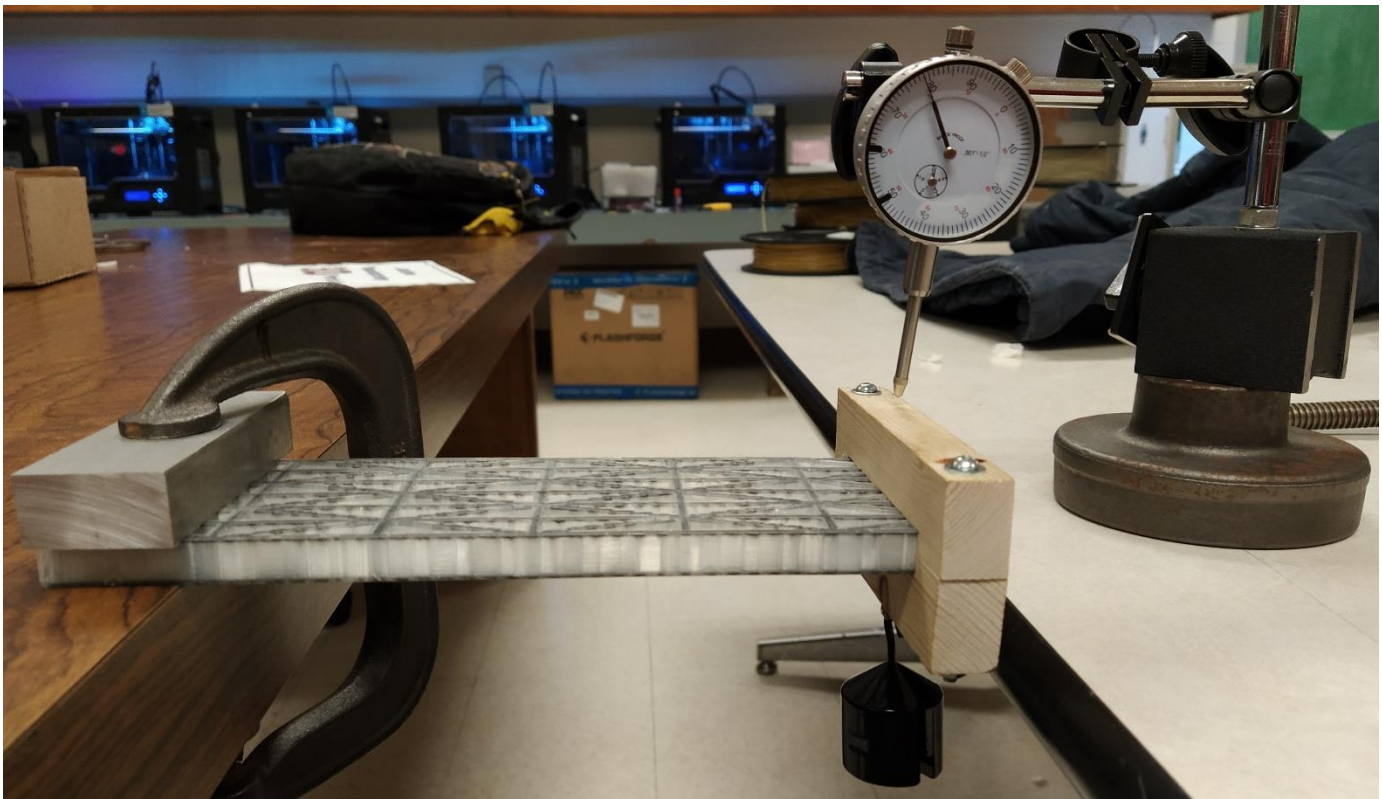
Figure 37 Cantilvered Beam Test Setup

To apply load onto the test piece, a fixture was used, that had previously been manufactured by previous graduate student. The fixture has a slot carved into each block, which are clamped onto the test piece with screws. There is also a hook on the bottom of the fixture, where a weight can be hung to apply load onto the test piece.

The masses used in the experiment are pictured below. Five progressively larger masses were used. The masses and the resultant weights are presented in a tabulated form. The smallest mass was 50 grams, which had a weight of 0.491 N. The largest mass used was 1000 grams (1 kg) and resultant force was 9.81 N. The 9.81 N load was used to compare results to the analytical and FEM predictions.

Mass (gram)	Force(N)
50	0.4905
100	0.981
200	1.962
500	4.905
1000	9.81

Figure 38 Masses used in experiment

To obtain deflection readings, the masses were loaded onto the hook, then the dial indicator gauge was brought into contact with the top surface of the fixture. Then, the dial was set to zero and the mass was removed, after which the test piece would spring back. The dial indicator reading was then recorded.

4) Results and Discussion

Stiffened grids were successfully printed, however there were many kinds of print errors, such as fiber misplacement, delamination, burns and curling. Analytical and experimental results were close to each other for cantilevered loading and suggests correlation. However, the simply supported experiment has not yet been performed. FEM analysis results did not agree with the experimental and analytical results. The FEM deflection prediction was half that of the analytical or experimental deflection.

4.1) Manufacturing

Several stiffened grids were printed successfully, but all of them had some form of observable printing errors. Two example are shown in photos.

Figure 39 Grid angled grid superimposed on orthogrid
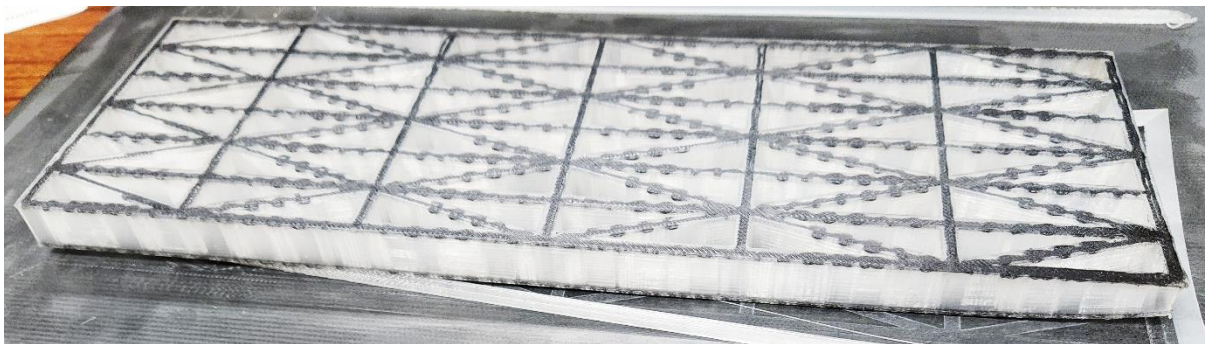
Figure 40 Orthotropic grid, on composite build plate

The major limitation of the Eiger software, is the lack of control over fiber orientation and placement. The Eiger software does not have the ability to place individual fiber strands, and has limited capability of placing fibers along curved paths. To elaborate, it is impossible to embed individual strands, or grouped strands within a layer of nylon. Either the entire layer must be carbon-nylon composite, or it must be pure nylon. Workarounds for these issues include having raised feature where the software may be instructed to use carbon fiber. However for more complicated geometry this does not work reliably.

Figure 41 Fiber discontinuity and curling

There were also numerous, and very consistent problems that caused a very high failure rate while printing parts. The parts often curl and become detached from the build plate. Even if the part does not curl during printing, the part may curl *after* it is removed from the plate, due to heat distortion. The two photos below display curling in both the longitudinal and lateral planes. The

part is an orthotropic grid that was printed without a skin, but a brim was used. One end of the part had lifted up due to curling.
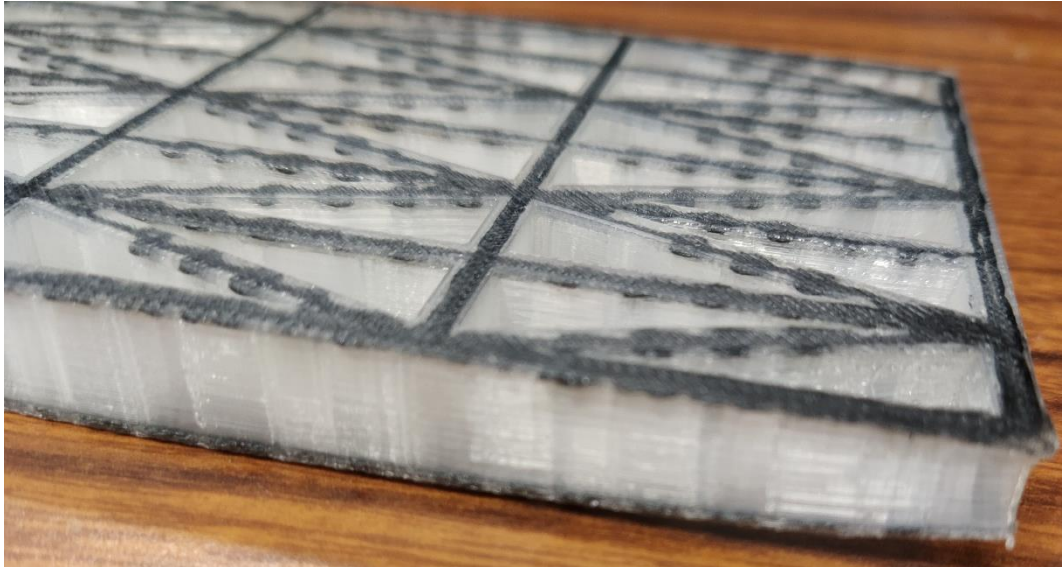
Figure 42Curling along the length
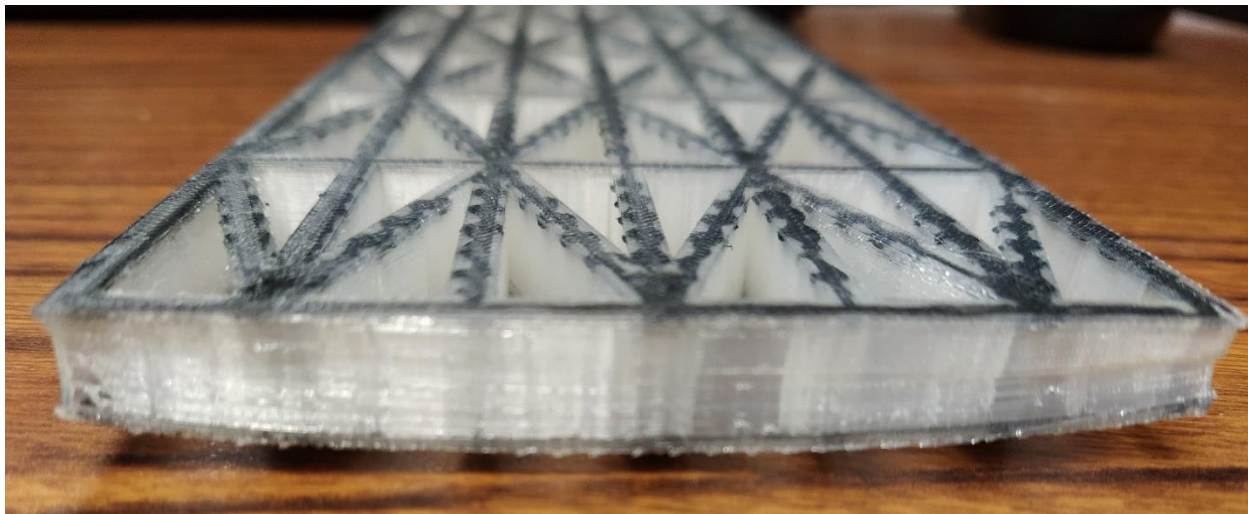
Figure 43 Curling along width

When observed from the front, it was seen that the corners had curled more than the center. Thus lateral curling had also occurred. Also the parts are prone to bond failures, where layers of nylon would not adhere during printing, and strings of material may stick out of the finished part. In many cases, the printer cannot detect this failure and continues the print operation. This may

cause the print head to gum up with nylon, because the material accumulates without being deposited onto the part. The carbon fiber also fails to bond with the nylon on occasion. Furthermore, almost every print has some degree of burning on the part. There were numerous times that the burns were so bad that the prints failed, or had to be discarded even when the print was completed.

Both bond failure and burning can be noticed on the pictures. It should be noted that in this case, the failures were minor and did not cause the entire print to fail. However, it should also be noted that these failures occur in almost every part and as such, these examples represent the best case scenario for consistent performance.

4.2) Analytical Deflection Prediction

The most significant results for analytically predicting the stiffness and thus, the deflection for the stiffener grid was the calculation of grid matrices. Once the matrices were calculated, other properties could be predicted. Matrices [A] and [D] for the whole grid (with carbon and nylon segments summed) are:

$$
\text{Atotal} = \begin{bmatrix} 77188.75323415 & 3904.34331575 & 0 \\ 3904.34331575 & 33798.28299308 & 0 \\ 0 & 0 & 3904.34331575 \end{bmatrix}
$$

$$
\text{Dtotal} = \begin{bmatrix} 0.08609656 & 0.00021072 & 0 \\ 0.00021072 & 0.02227988 & 0 \\ 0 & 0 & 0.02603088 \end{bmatrix}
$$

The bending stiffness was calculated to be 7.289 N m^2. Deflection for cantilevered beam was calculated to be 0.00392m, or 3.92mm. Deflection for simply supported beam was calculated to be 0.000158m or 0.158mm.

4.3) Optistruct deflection prediction

The maximum simulated deflection for the cantilevered beam was 1.97mm. This was less than the analytical deflection prediction by approximately 50%, however it was within the same order of magnitude. As expected, the maximum deflection for the simply supported beam was at the middle. The maximum value was 0.093mm. Again, this was less than the analytical prediction for the same loading and supports, but they were in the same order of magnitude.

4.4) Experimental Results

For the cantilevered beam, the maximum deflection was 3.84mm, which agrees very closely with the analytical prediction of 3.92mm. The experimental deflection was 2% lower than analytical. Compared to the Optistruct analysis, the experimental result showed a 48% great deflection. However, it should be noted that the experimental method was very basic and more sophisticated methods should be used in the future.

Table 9 Forces and Deflections

Force(N)	Deflection (mm)
0.4905	0.2032
0.981	0.3556
1.962	0.7112
4.905	1.8542
9.81	3.8354

Table 10 Deflection Comparison

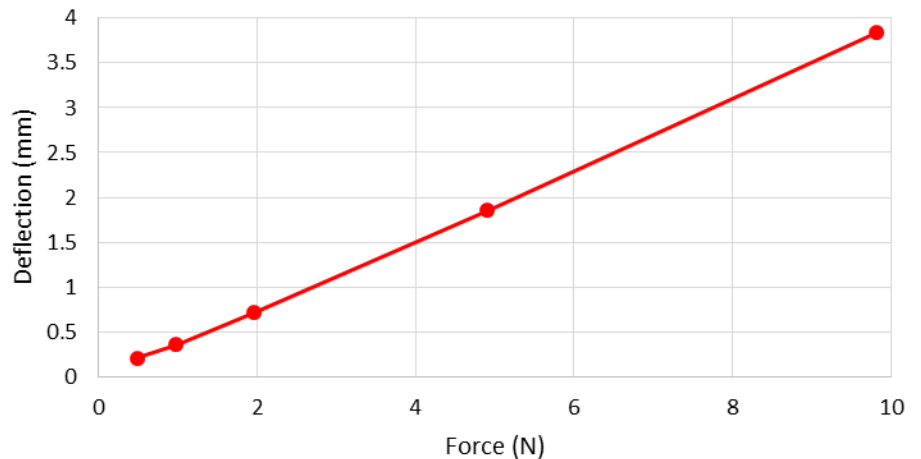| Method	Deflection (mm)
Analytical	3.92
Optistruct	1.97
Experimental	3.84

Figure 44 Force vs. Deflection

5) Conclusion

The ability of the Markforged Mark Two printer to manufacture parts with continuous carbon fiber was used to develop a methodology of printing stiffened grids for thin plates. Subsequently, the properties of the grids were investigated analytically, experimentally and computationally. To manufacture stiffened grids, it was necessary to determine how to manipulate the software into laying fiber along desired directions, on the top and bottom of thin ribs. The minimum rib width had to be determined through experimental trial and error, since fiber cannot be placed on ribs that are too thin. Next, the specific settings in the slicing software had to be determined. The key setting was found to be fiber angle of the 'isotropic fiber' option (the name is a misnomer because an individual layer of fiber cannot be isotropic). For any layer, the angle of the fiber must be equal to the angle of the ribs. Furthermore, it was found that the Mark Two can print geometry much thinner than the recommended settings. For example the walls were recommended to be two layers thick, but it was possible to consistently print ribs that were only a single layer thick, and there could be as little as three percent infill.

Another significant achievement was the development of an analytical method to obtain the laminate stiffness matrices for the stiffened grids. Because there was carbon on the top and bottom, and the layers were equidistant apart from the centroid, the grids could be treated abstractly as symmetric laminates, which greatly simplified analysis. Prior work done by Tsai-Chen provided a formulation to obtain stiffness matrices, provided that moments of inertia were available for the ribs. The moments of inertia of the nylon and carbon sections of the ribs were calculated separately, which were then used to calculated stiffness matrices for nylon and carbon segments. The matrices were summed to obtain total stiffness matrices for the grids, which were then used to predict deflection for a 9.81 Newton load (1kg hanging mass), using an equation from the PhD dissertation

of Rios, a previous UTA student. The predicted deflection for the test grid in cantilevered loading was 3.92mm. With the same load and simply supported, the grid was predicted to have 0.158mm of deflection.

Furthermore, Altair HyperWorks was used to predict deflection with FEM analysis. Since the nylon segments of the grid were very thin, shell models were used. Shell models have two dimensional elements, and the thickness can be set as a parameter. For the simulating the carbon segments, one dimensional rod elements were used, since the thin lines of carbon only contribute stiffness in bending. Cantilevered deflection prediction for 9.81N load was 1.97mm, and simply supported grid deflection for the same load was 0.093mm.

The cantilevered deflection experiment was performed using simple apparatus. The grid was fixed to the side of the table by using a C-clamp and loaded on the other end using a series of weights, which were hung from a fixture. Maximum experimental deflection with 9.81N load was 3.84mm, which agrees very closely with the analytical prediction of 3.92mm.

For future work, a heated build plate should be considered in order to improve the build quality of parts printed with the Markforged Mark Two. At least one of the older build plates could be modified to have heating elements installed, which would possibly reduce curling of parts due to distortion while cooling, and improve adhesion of parts to the build plate. Another objective would be to develop a method for printing optimized grids. Optimized grids tend to have organic shaped ribs. The problem encountered with printing such shapes was that it was impossible to instruct Eiger to put carbon fiber along the correct paths. A solution to this problem should be investigated. Related to this, the problems with fiber placement such as breaks in the fibers, or curling should also be solved. There is also potential to use ONYX instead of nylon. ONYX has chopped carbon fiber within the plastic filament, which enhances

strength and stiffness. It is also possible to embed continuous carbon fibers within ONYX parts, in the same way as was done with nylon.

Further testing needs to be done, with proper test machines and fixtures instead of low budget improvised devices. The tests already performed indicates that the analytical method of stiffness prediction provides good results, however there should be further investigation. If optimized grids can be printed, there should also be testing done for such parts.

The FEM analysis provided inaccurate results. Although the deflections were in the same order of magnitude, the predictions were off by about fifty percent. This analysis should be redone and the cause of the discrepancy found and corrected. The most likely source of error is within the carbon elements and material properties, since they dominate stiffness.

References

[1] Gere, J. M., and Goodno, B. J., *Mechanics of materials*, Toronto: Cengage Learning, 2010.

[2] Chen, H.-J., and Tsai, S. W., "*Analysis and Optimum Design of Composite Grid Structures*," *Journal of Composite Materials*, vol. 30, 1996, pp. 503–534.

[3] Daniel, I. M., and Ishai, O., *Engineering mechanics of composite materials*, Oxford University Press, 2007.

[4] Rios, G., "*A Unified Analysis of Stiffener Reinforced Composite Beams with Arbitrary Cross-Section*," 2009.

[5] *Practical Aspects of Finite Element Analysis*, Troy, Michigan: Altair Engineering, 2019

[6] "3D Printer Types & Technologies," *Markforged Industrial Strength 3D Printing* Available: https://markforged.com/learn/3d-printer-types-technologies

[7] SD3D Printing, "Best Rapid Prototyping Solution? SLA vs. SLS vs. FFF," *SD3D Printing* Available: https://www.sd3d.com/fff-vs-sla-vs-sls/

[8] "Markforged Materials Data Sheet - 2017 1 / 2" Available: https://www.3diligent.com/wp-content/uploads/2017/08/markforged_materials_datasheet.pdf.

[9] "3D Printer Types & Technologies," *Markforged Industrial Strength 3D Printing* Available: https://markforged.com/learn/3d-printer-types-technologies/.

[10] "3D Printing Settings Impacting Part Strength." *Markforged Industrial Strength 3D Printing*, https://markforged.com/learn/3d-printing-settings-impacting-part-strength/.

[11] Megson, T. H. G., *Aircraft sturctures for engineering students*, Amsterdam: Elsvier, 2007.

Appendix

rib_stiffness_matrices

October 12, 2019

In [2]: *#parallel ribs, square grid*

import numpy as np from numpy.linalg import *
angle=22.3 *#degrees, horizontal ribs*
th=np.deg2rad(angle) *#convert angle to radians*
Ex_nylon = 0.94*(10**9) *#0.94 gigapascals*
Es_nylon =0.84*(10**9) *#0.84 gigapascals*
Ex_carbon= 54*(10**9) *#54 gigapascal*
Es_carbon=51*(10**9)   *#51 gigapascal*

In [3]: *#outer rib dimensions*
h1 = 0.5*0.0254   *#inches to meters*
w1 = 2.69/1000 *#mm to meters*
t1 = 3*(0.125)/1000   *# thickness of the roof and
floor layers, 0.125 mm per layer*

t3= 0.65/1000   *# wall thickness 0.65 mm converted
to meters*

#composite layer dimensions
 t2 = 0.125/1000   *#single layer thickness, 0.125mm
to meters*

h2 = h1 - 2*t1
w3= 1/1000 *#w3 is approx 1 mm*

#inner cavity dimensions
h3 = h2-2*t2
w2 = w1 - 2*t3

#ribs lengths
d0 =12.55/1000
d90=40.88/1000
dth =42.77/1000

In [4]: *#beam dimensions*

L_beam = 10*0.0254

```
#inch to meters
w_beam = 3.333*0.0254
```

In [5]: h1

Out[5]: 0.0127

In [6]: h2

Out[6]: 0.011949999999999999

In [7]: h3

Out[7]: 0.011699999999999999

In [8]: w1

Out[8]: 0.00269

In [9]: w2

Out[9]: 0.0013900000000000002

In [10]: w3

Out[10]: 0.001

In [11]: t1

Out[11]: 0.000375

In [12]: t2

Out[12]: 0.000125

In [13]: t3

Out[13]: 0.00065

In [14]:
```
def Iy( y,z,d ):
    A=y*z
```

```python
    Iy = (y*z**3)/12 + A*d**2
    return Iy




def Iz( y,z,d ):
    A=y*z
    Iz=(z*y**3)/12 + A*d**2
    return Iz




# function definitions to calculate A and B matrix

def D_matrix( Iy,Iz,Ex,Es,angle ):

    m = np.cos(angle)
    n = np.sin(angle)

    I0 = Iy     #remember, bending around the x axis
    Ith = Iy
    I90=Iy

    J0= Iy+Iz
    J90=Iy+Iz
    Jth =Iy+Iz

    D11 = Ex*I0/d0 + 2*Ex*Ith*(m**4)/dth + 2*Es*Jth*(m**2)*(n**2)/dth
    D12 = 2*Ex*Ith*(m**2)*(n**2)/dth - 2*Es*Jth*(m**2)*(n**2)/dth
    D13=0
    D21 = D12
    D22 = Ex*I90/d90 + 2*Ex*Ith*(n**4)/dth + 2*Es*Jth*(m**2)*(n**2)/dth
    D23=0
    D31 = 0
    D32=0
    D66 = 2*Ex*Ith*(m**2)*(n**2)/dth + Es*J0/(4*d0) + Es*J90/(4*d90) + (Es*Jth*((m**2)

    D = np.array([ [ D11,D12,D13],[ D21,D22,D23],[ D31,D32,D 66]])
    return D

def A_matrix( Ex,Es,rib_height,rib_width,angle ):
```

```python
    m = np.cos(angle)
    n = np.sin(angle)

    A90=Ath=A0=rib_height*rib_width #in this case, because cross section of flat, upr

    A11=Ex*A0/d0 + 2*Ex*Ath*(m**4) /dth
    A12= 2*Ex*Ath*(m**2)*(n**2)/dth
    A13= 0
    A21= 2*Ex*Ath*(m**2)*(n**2)/dth
    A22= 2*Ex*A90/d90 + 2*Ex*Ath*(n**4)/dth
    A23= 0
    A31= 0
    A32= 0
    A33= 2*Ex*Ath*(m**2)*(n**2)/dth


    A = np.array([ [ A11,A12,A13],[ A21,A22,A23],[A31,A32,A33] ])
    return A
```

In [15]:
#heights,width,x displacement,y displacemnt of the discrete rectangles
I and J are the carbon portions

```python
hA=h1
hB=h1/2 - h2/2
hC=h1/2 - h2/2
hD=h1
hE=h2/2 - h3/2
hF= h2/2 - h3/2
hG= h2/2 - h3/2
hH= h2/2 - h3/2
hI= h2/2 - h3/2
hJ= h2/2 - h3/2
```

In [16]: hA
Out[16]: 0.0127

In [17]: hB
Out[17]: 0.0003750000000000033

In [18]: hC
Out[18]: 0.0003750000000000033

In [19]: hD
Out[19]: 0.0127

In [20]: hE
Out[20]: 0.0001250000000000001

In [21]: hF
Out[21]: 0.0001250000000000001

In [22]: hG
Out[22]: 0.0001250000000000001

In [23]: hH
Out[23]: 0.0001250000000000001

In [24]: hI
Out[24]: 0.0001250000000000001

In [25]: hJ
Out[25]: 0.0001250000000000001

In[26]:

wA= w1/2 –
w2/2

wB= w2
wC= w2
wD=w1/2 -
w2/2

wE= w2/2 -
w3/2
wF= w2/2 -
w3/2
wG= w2/2 -
w3/2
wH= w2/2 -
w3/2
wI= w3
wJ= w3

In [27]: wA
Out[27]: 0.00065

In [28]: wB
Out[28]: 0.0013900000000000002

In [29]: wC
Out[29]: 0.0013900000000000002

In [30]: wD
Out[30]: 0.00065

In [31]: wE
Out[31]: 0.00019500000000000008

In [32]: wF
Out[32]: 0.00019500000000000008

In [33]: wG
Out[33]: 0.00019500000000000008

In [34]: wH
Out[34]: 0.00019500000000000008

In [35]: wI
Out[35]: 0.001

In [36]: wJ
Out[36]: 0.001

In [37]:
yA= w1/2 - t3/2
 yB= 0
 yC= 0
yD= w1/2 - t3/2
yE= w3/2 + (w2/2 - w3/2)/2
yF= w3/2 + (w2/2 - w3/2)/2
yG= w3/2 + (w2/2 - w3/2)/2
yH= w3/2 + (w2/2 - w3/2)/2
yI= 0
yJ= 0

In [38]: yA
Out[38]: 0.00102

In [39]: yB
Out[39]: 0

In [40]: yC
Out[40]: 0

In [41]: yD

In [42]: yE
Out[42]: 0.0005975

In [43]: yF
Out[43]: 0.0005975

In [44]: yG
Out[44]: 0.0005975

In [45]: yH
Out[45]: 0.0005975

In [46]: yI
Out[46]: 0

In [47]: yJ
Out[47]: 0

In [48]:
zA= 0
zB= h1/2 -t1/2
zC= h1/2 -t1/2
zD= 0
zE= h2/2 -
t2/2
zF= h2/2 -
t2/2
zG=h2/2 - t2/2
zH=h2/2 - t2/2
zI=h2/2 - t2/2
zJ=h2/2 - t2/2

In [49]: zA
Out[49]: 0

In [50]: zB
Out[50]: 0.0061625

In [51]: zC
Out[51]: 0.0061625

In [52]: zD
Out[52]: 0

In [53]: zE
Out[53]: 0.005912499999999999

In [54]: zF
Out[54]: 0.005912499999999999

In [55]: zG
Out[55]: 0.005912499999999999

In [56]: zH
Out[56]: 0.005912499999999999

In [57]: zI
Out[57]: 0.005912499999999999

In [58]: zJ
Out[58]: 0.005912499999999999

In [59]:
IAy=Iy(wA,hA,zA)

IBy=Iy(wB,hB,zB)

ICy=Iy(wC,hC,zC)

IDy=Iy(wD,hD,zD)

IEy=Iy(wE,hE,zE)

IFy=Iy(wF,hF,zF)

IGy=Iy(wG,hG,zG)

IHy=Iy(wH,hH,zH)

Iy_nylon = IAy+IBy+ICy+IDy+IEy+IFy+IGy+IHy

In [60]: IAy
Out[60]: 1.1095407916666665e-10

In [61]: IBy
Out[61]: 1.9801310156250016e-11

In [62]: Icy
Out[62]: 1.9801310156250016e-11

In [63]: IDy
Out[63]: 1.1095407916666665e-10

In [64]: IEy
Out[64]: 8.521246093750009e-13

In [65]: IFy
Out[65]: 8.521246093750009e-13

In [66]: IGy
Out[66]: 8.521246093750009e-13

In [67]: IHy
Out[67]: 8.521246093750009e-13

In [68]: Iy_nylon
Out[68]: 2.6491927708333324e-10

In [69]:
 IAz=Iz(wA,hA,yA)

IBz=Iz(wB,hB,yB)

ICz=Iz(wC,hC,yC)

IDz=Iz(wD,hD,yD)

IEz=Iz(wE,hE,yE)

IFz=Iz(wF,hF,yF)

IGz=Iz(wG,hG,yG)

IHz=Iz(wH,hH,yH)

Iz_nylon = IAz+IBz+ICz+IDz+IEz+IFz+IGz+IHz

In [70]: IAz
Out[70]: 8.879146791666669e-12

In [71]: IBz
Out[71]: 8.392559375000011e-14

In [72]: ICz
Out[72]: 8.392559375000011e-14

In [73]: IDz
Out[73]: 8.879146791666669e-12

In [74]: IEz
Out[74]: 8.779265625000013e-15

In [75]: IFz
Out[75]: 8.779265625000013e-15

In [76]: IGz
Out[76]: 8.779265625000013e-15

In [77]: IHz
Out[77]: 8.779265625000013e-15

In [78]: Iz_nylon
Out[78]: 1.7961261833333333e-11

In [79]:
IIy=Iy(wI,hI,zI)

IJy=Iy(wJ,hJ,zJ)
Iy_carbon = IIy+IJy

In [80]: IIy
Out[80]: 4.369869791666669e-12

In [81]: IJy
Out[81]: 4.369869791666669e-12

In [82]: Iy_carbon
Out[82]: 8.739739583333338e-12

In [83]:
IIz=Iz(wI,hI,yI)

IJz=Iz(wJ,hJ,yJ)
Iz_carbon = IIz+IJz

In [84]: IIz
Out[84]: 1.0416666666666676e-14

In [85]: IJz
Out[85]: 1.0416666666666676e-14

In [86]: Iz_carbon
Out[86]: 2.0833333333333353e-14

In [87]: *#total moment of inertia*

Iy_total = Iy_carbon+Iy_nylon

Iz_total = Iz_nylon + Iz_carbon

In [88]: Iy_total
Out[88]: 2.736590166666666e-10

In [89]: Iz_total
Out[89]: 1.7982095166666667e-11

In [90]:

A_nylon = A_matrix(Ex_nylon,Es_nylon,h1,w1,th)

A_carbon = A_matrix(Ex_carbon,Es_carbon,h2,w3,th)

D_nylon = D_matrix(Iy_nylon,Iz_nylon,Ex_nylon,Es_nylon,th)

D_carbon = D_matrix(Iy_carbon,Iz_carbon,Ex_carbon,Es_carbon,th)

A_total = A_nylon + A_carbon

D_total = D_nylon+D_carbon

a_total = inv(A_total)

d_total = inv(D_total)

In [91]: A_nylon

Out[91]: array([[3659183.70198603,   185087.96721469,   0.],
        [185087.96721469,   1602229.87289643,   0.],
        [0. ,   0. ,   185087.96721469]])

In [92]: A_carbon

Out[92]: array([[73529569.53216098,   3719255.34853372,   0.],
        [3719255.34853372, 32196053.1201813 ,   0.],
        [0. ,   0. ,   3719255.34853372]])

In [93]: D_nylon

Out[93]: array([[29.74493188, 0.06573087, 0.] ,
            [0.06573087, 7.70255725, 0.] ,
            [0. ,   0. ,   9.03022117]])

In [94]: D_carbon
Out[94]: array([[56.35162687, 0.14499343, 0.] ,
            [0.14499343, 14.57732346, 0.] ,
            [0. ,   0. , 17.00065993]])

In [95]: A_total
Out[95]: array([[77188753.23414701, 3904343.31574841, 0.] ,
            [3904343.31574841, 33798282.99307773,   0.] ,
            [0. ,   0. ,   3904343.31574841]])

In [96]: D_total
Out[96]: array([[86.09655875, 0.2107243 , 0.] ,
            [0.2107243 , 22.27988071,   0.] ,
            [0. ,   0. , 26.0308811]])

In [97]: a_total
Out[97]: array([[1.30313997e-08, -1.50537406e-09,   0.00000000e+00] ,
            [-1.50537406e-09, 2.97612011e-08, 0.00000000e+00] ,
            [0.00000000e+00, 0.00000000e+00, 2.56125017e-07]])

In [98]: d_total
Out[98]: array([[0.01161513, -0.00010986, 0.] ,
            [-0.00010986, 0.04488458, 0.] ,
            [0. , 0., 0.03841591]])

In [99]: *#beam bending stiffness*
flex_wide = w_beam*D_total[0][0]

In [100: flex_wide
Out[100]: 7.289

cantilevered deflection

In [15]:

```
P = 9.81
L = 8.50*0.0254
a = 7.75* 0.0254
flex_wide = 7.289
deflection_max = P*a**2*(3*L - a)/(6*flex_wide)
```

In [16]: deflection_max

Out[16]: 0.003918796568002384

simply_supported

In [1]:
flex_wide=7.289
P = 9.81
L= 7*0.0254
deflection_max =(P*L**3)/(48*flex_wide)

In [4]: deflection_max

Out[4]: 0.00015759959230552886